doi:10.1006/jmbi.2001.5385 available online at http://www.idealibrary.com on IDEAL® J. Mol. Biol. (2002) 317, 291–308

JMB

Twist and Shear in β-Sheets and β-Ribbons

Bosco K. Ho and Paul M. G. Curmi*

Initiative in Biomolecular Structure (IBiS), School of Physics, University of New South Wales, Sydney 2052, Australia

The structures of the β-sheets and the β-ribbons have been analysed using high-resolution protein structure data. Systematic asymmetries measured in both parallel and antiparallel β-structures include the sheet twist and the strand shear. In order to determine the origin of these asymmetries, numerous interactions and correlations were examined. The strongest correlations are observed for residues in antiparallel β-sheets and β-ribbons that form non-H-bonded pairs. For these residues, the sheet twist is correlated to the backbone ϕ angle but not to the ψ angle. Our analysis supports the existence of an inter-strand $C^{\alpha}H^{\alpha}\cdots O$ weak H-bond, which, together with the $CO\cdots HN$ H-bond, constitutes a bifurcated H-bond that links neighbouring β-strands. Residues of β-sheets and β-ribbons in high-resolution protein structures form a distinct region of the Ramachandran plot, which is determined by the formation of the bifurcated H-bond, the formation of an intra-strand $O\cdots H^{\alpha}$ non-bonded polar interaction, and an intra-strand $O\cdots C^{\beta}$ steric clash. Using β-strands parameterised by ϕ-ψ values from the allowed β-sheet region of the Ramachandran plot, the shear and the right-hand twist can be reproduced in a simple model of the antiparallel and parallel β-ribbon that models the bifurcated H-bonds specifically. The conformations of interior residues of β-sheets are shown to be subsets of the conformations of residues of β-ribbons.

Keywords: β-sheet; twist; shear; bifurcated hydrogen bond; Ramachandran plot

*Corresponding author

Introduction

The structure of the β-sheet was predicted by Linus Pauling[1] in 1951 by considering planar peptide units, steric clashes and $CO\cdots HN$ H-bonds. Although the Pauling β-sheet is accurate in many respects, several structural properties have been observed that are not found in the Pauling β-sheet: the shear, the right-hand twist and the $C^{\alpha}H^{\alpha}\cdots O$ weak H-bonds.

Pauling assumed that in the antiparallel β-sheet, linear $CO\cdots NH$ H-bonds form between the strands, which aligns neighbouring strands (Figure 1(a)). However, in 1973, Fraser & MacRae[2] found that in actual antiparallel β-sheets the strands have slipped along the N to C-terminal backbone direction with respect to neighbouring strands (Figure 1(b)).[3,4] We call this property the shear of the antiparallel β-sheet. The shearing in antiparallel β-sheets has been shown[4] to produce non-linear $CO\cdots HN$ H-bonds.[5,6]

Ramachandran showed that intra-strand steric clashes[7] result in allowed regions of the ϕ-ψ plot (Figure 2(a)), which can be accounted for accurately using Lennard-Jones potentials and electrostatics.[8] However, the region of the ϕ-ψ plot containing residues in β-sheets (Figure 2(a)), as defined by H-bonds,[9] is significantly smaller than the traditional β-region of the Ramachandran plot of all residues.[10]

Although the concept of the $CH\cdots O$ weak H-bond has been around for some time,[11] the existence of the $CH\cdots O$ weak H-bond was not demonstrated until Taylor & Kennard[12] exhaustively analysed $CH\cdots O$ contacts in structures of organic molecules that had been determined by neutron diffraction. Subsequently, Derewenda and co-workers[13] examined the $CH\cdots O$ contact in high-resolution protein structures and found systematic $C^{\alpha}H^{\alpha}\cdots O$ H-bonds in both parallel and antiparallel β-sheets.

First observed by Chothia[14] in 1973, one of the most striking properties of β-sheets is the predomi-

Abbreviations used: H bond, hydrogen bond; corr-, correlation coefficient.

E-mail address of the corresponding author: p.curmi@unsw.edu.au

0022-2836/02/020291–18 $35.00/0

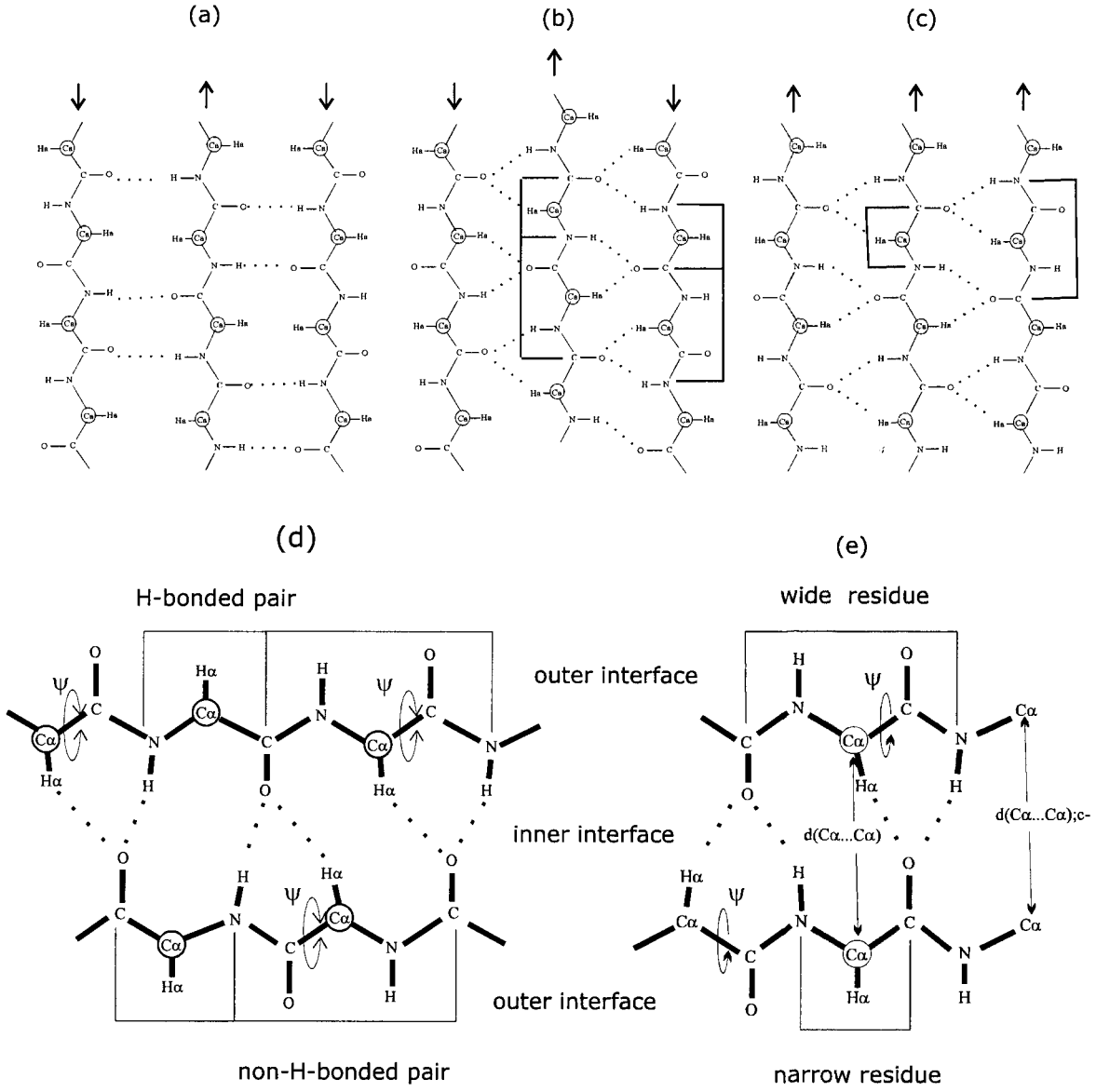

Figure 1. The different types of β-sheets and inter-strand pairs. (a) The Pauling antiparallel β-sheet. (b) The sheared antiparallel β-sheet, where the box encloses an H-bonded (above) and non-H-bonded (below) inter-strand pair. (c) The parallel β-sheet where the box encloses a parallel inter-strand pair. Once the bifurcated H-bonds are included, the sheared antiparallel β-sheet (b) resembles the parallel β-sheet (c). (d) A detailed schematic of the H-bonded pair (left box) coupled to the neighbouring non-H-bonded pair (right box) where the labelled ψ angles (illustrated) all take on the same value in the model. (e) A detailed schematic of the parallel pair where the ψ angle on the left is assumed to take on the same value as the other labelled ψ angle.

nance of the right-hand twist. Previous explanations for the right-hand twist have sought a bias in the twisting of isolated β-strands: entropy biasing the centroid of the sterically allowed region of the Ramachandran plot;[14] intra-strand van der Waals interactions involving side-chain;[15] intra-strand $O\cdots C^{\beta}$ steric clashes;[16] long-range intra-strand electrostatics;[17] and the difference between the N-C^{α} and C-C^{α} bonds torsional potentials.[18] However, isolated β-strands in molecular dynamics simulations are not twisted,[19] suggesting that the stabilisation of the right-hand twist must be due to inter-strand interactions. Another study found that inter-strand electrostatic interactions induce a right-hand twist, although a specific mechanism was not given.[20]

We have made systematic measurements of the twist and the shear of β-sheets and β-ribbons using high-resolution structures. We have measured the high-resolution β-sheet region of the Ramachandran plot and identified the interactions that constrain this region, in particular, the intra-strand $O\cdots C^{\beta}$ steric clash that results in the residues of β-structures residing in an asymmetric region of the Ramachandran plot. By using a simple model of the antiparallel β-ribbon using bifurcated hydro-

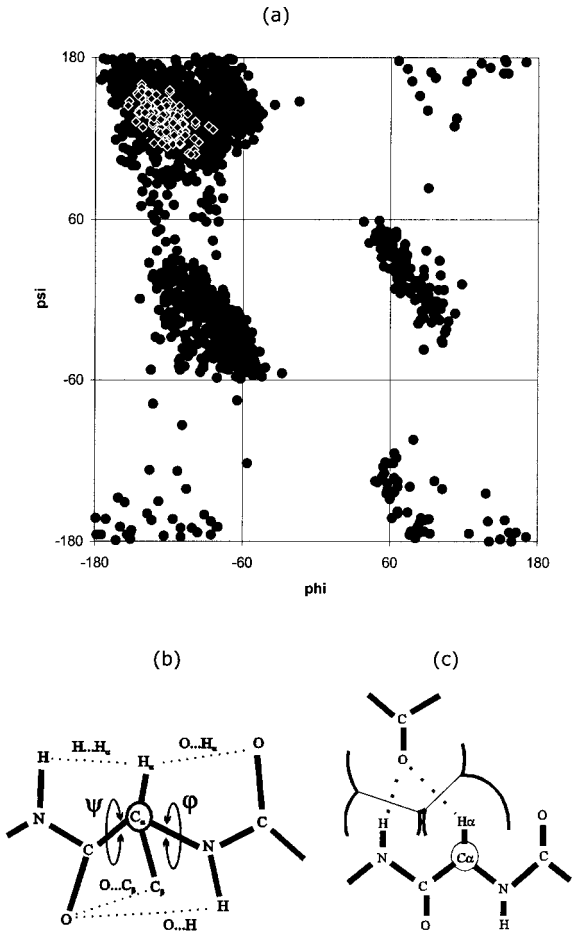

Figure 2. The ϕ-ψ dihedral angles. (a) Ramachandran plot of all residues (●) taken from structures in the PDB with resolution better than <1.3 Å. Residues from β-sheets are shown as (◇). (b) A schematic of the backbone showing how the intra-strand $H\cdots H^{\alpha}$ and $O\cdots C^{\beta}$ distances are parameterised by ψ; and the $O\cdots H^{\alpha}$ distance is parameterised by ϕ. (c) The bifurcated H-bond where the O atom forces the H and H^{α} atoms into steric contact.

gen bonds, we show that there is an intimate connection between the β-sheet region of the Ramachandran plot, the twist and the shear. The right-handed twist is a result of the asymmetry in the Ramachandran plot, and the shear is a result of the bifurcated H-bond. Our model reproduces the observed values of shear and right-hand twist of the β-sheet as well as the correlations between parameters.

Results

β-Sheets and β-ribbons

Residues were defined as belonging to β-structures using the program DSSP.[9] The β-ribbon residues were differentiated from β-sheet residues, as β-ribbons tend to form coiled-coils, whereas β-sheets form flatter, sheet-like structure.[21] Edge residues of β-sheets can form coiled-coils, like β-ribbons.[21] In order to differentiate β-ribbons from β-sheets, we have used only interior β-sheet residues for the β-sheet statistics, eliminating edge strand residues. We have taken measurements from a non-redundant data set of high-resolution protein structures, which includes reliable positions for both the amide and aliphatic hydrogen atoms (see Methods).

Inter-strand pairs

We have measured the β-sheets and β-ribbons in terms of inter-strand pairs of residues: adjacent pairs of residues on neighbouring β-strands. There are two different types of inter-strand pairs in anti-parallel β-sheets:[20] H-bonded and non-H-bonded pairs (Figure 1(d)). In H-bonded pair residues (left box in Figure 1(d)), the CO group of one residue forms an H-bond with the NH group of the other residue. In non-H-bonded pair residues (right box in Figure 1(d)), the CO and NH groups of the two residues point away from each other. Two non-H-bonded pairs flank every H-bonded pair and both the H-bonded pair and the non-H-bonded pair possess local dyad symmetry (Figure 1(d)).

There is only one type of inter-strand pair in parallel β-sheets: the parallel pair (Figure 1(e)). As the parallel pair does not possess dyad symmetry, each residue in a parallel pair is distinct. In the narrow bonding residue (bottom residue in Figure 1(e)), the CO and NH groups form H-bonds with residues on the other strand. In the wide bonding residue (top residue in Figure 1(e)), the CO and NH groups point away from the other residue and it is the CO and NH groups of the intra-strand neighbours of the wide residue that form H-bonds with the CO and NH groups of the narrow residue. Neighbouring parallel pairs are orientated in opposite directions (Figure 1(c)).

Shear

Fraser & McRae[2] originally defined the shear in terms of the unit cell of the crystal structure of poly-L-alanine. This definition is unsatisfactory, as it depends on the underlying crystallographic parameters and not on the stereochemistry of the β-sheet. MacCallum and co-workers[4] defined the shear in terms of the non-linearity of the $CO\cdots HN$ H-bond, and Shamovsky and co-workers[18] defined the shear as the ratio of inter-strand $d(O\cdots O)$ to $d(H\cdots H)$ between residues on adjacent β-strands. In both these definitions, if there is a twisting of the β-sheet but no shearing, an apparent shear is produced. We have defined the shear in terms of inter-strand pairs, where the shear is the displacement of the C^{α} atom along the backbone direction (Figure 3(a); see Methods for a detailed description). This definition avoids the artefact due to twisting.

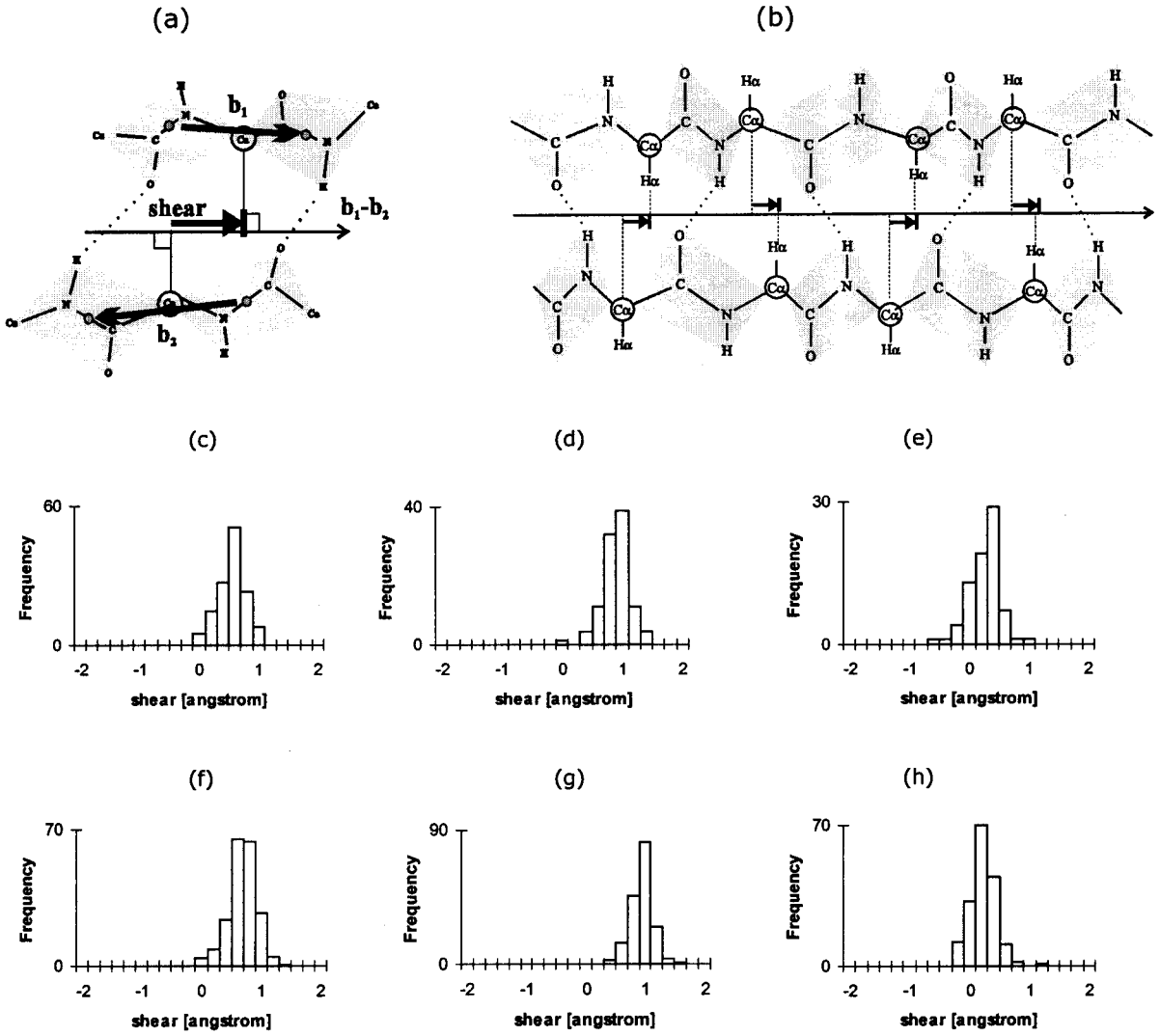

Figure 3. Shear of the inter-strand pairs. (a) Schematic of the shear of the antiparallel non-H-bonded pair. (b) A net positive shear of the parallel pairs results in an apparent compression and expansion of alternate peptide units in a parallel β-ribbon. The shear in β-ribbons for: (c) H-bonded pairs, 0.45(±0.25) Å; (d) non-H-bonded pairs, 0.80(±0.25) Å; and (e) parallel pairs, 0.18(±0.25) Å. The shear in β-sheets for: (f) H-bonded pairs, 0.58(±0.25) Å; (g) non-H-bonded pairs, 0.85(±0.25) Å; and (h) parallel pairs, 0.13(±0.25) Å.

The observed distributions of shear are positive and placed well away from zero (Figure 3(c)-(h)). The shear of the non-H-bonded pairs (antiparallel β-ribbon, Figure 3(d); antiparallel β-sheet, Figure 3(g)) is larger than the shear of the H-bonded pairs (antiparallel β-ribbon, Figure 3(c); antiparallel β-sheet, Figure 3(f)). The positive shear in both H-bonded and non-H-bonded pairs results in an asymmetric displacement of neighbouring strands, where each strand has been displaced towards its C-terminal end.

The observed shear in parallel β-ribbons (Figure 3(e)) and parallel β-sheets (Figure 3(h)) is also positive but smaller than in antiparallel structures. The net positive parallel shear does not correspond to the global shearing of the β-strands. As one moves along a pair of parallel strands, the wide and narrow residue types will alternate along the strand. Therefore, if average local shear is positive, each wide residue will be sheared towards the C terminus of its strand (Figure 3(b)). However, since successive wide residues alternate between strands, as one moves along the parallel β-ribbon, neither strand will have a net or global shear. A positive net shear corresponds to an apparent compression and extension of alternate peptide units along a strand. This could be due to peptide units twisting in three dimensions (Figure 4(a)).

Sheet twist

We have measured the twist in terms of the sheet twist, a geometric measure of the twisting of the β-sheet in terms of an inter-strand pair. The sheet twist is defined as the angle between the backbone vectors of the two residues in the pair

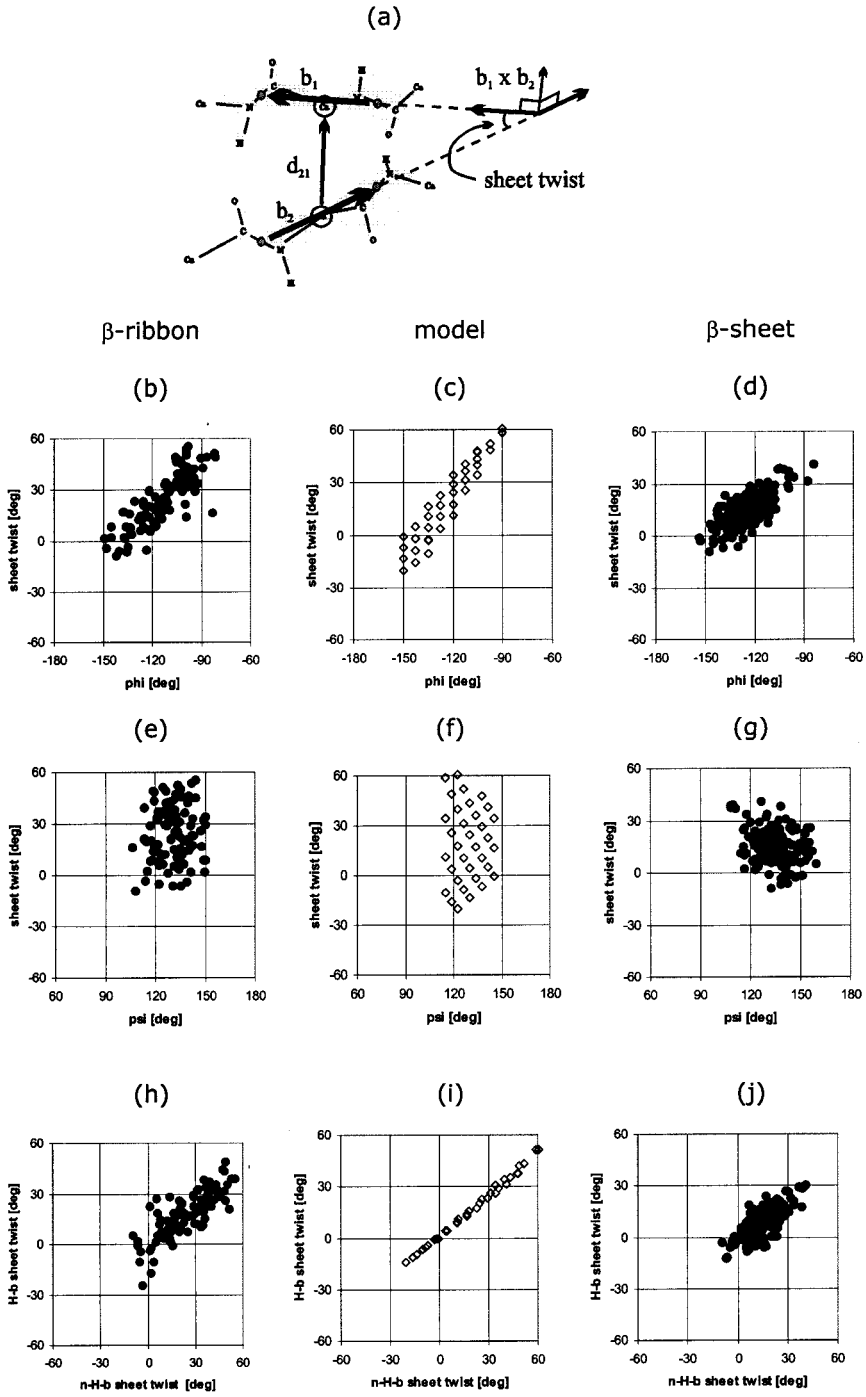

Figure 4. Sheet twist in the antiparallel inter-strand pairs. (a) Schematic of the sheet twist in the non-H-bonded pair. In the non-H-bonded pair, sheet twist *versus* ϕ in: (b) β-ribbon, slope 0.85, correlation coefficient (corr) 0.83; (c) model, slope 1.30, corr 0.96; and (d) β-sheet, slope 0.57, corr 0.74. In the non-H-bonded pair, sheet twist *versus* ψ in: (e) β-ribbon, (f) model and (g) β-sheet. H-bonded pair sheet twist *versus* non-H-bonded pair twist in: (h) β-ribbon, slope 0.68, corr 0.81; (i) model, slope 0.76, corr 0.98; and (j) β-sheet, slope 0.79, corr 0.73.

(Figure 4(a); see Methods for a detailed description). Since β-strands in a β-sheet are generally at a fixed distance apart, the magnitude of this angle is mainly due to the twisting of the β-strands.

The observed sheet twist (Table 1) is strongly positive, corresponding to a right-hand twist. The sheet twist in the antiparallel β-ribbon is ~10° larger than the sheet twist of the antiparallel β-sheet, and the standard deviation in the antiparallel β-ribbon non-H-bonded pair is 6° larger than the non-H-bonded pair in the antiparallel β-sheet. The parallel β-ribbon sheet twist is 5° greater than the parallel β-sheet sheet twist. These measurements reflect previous observations of the greater twist

Table 1. Parameters of the inter-strand pairs in observed β-sheets, observed β-ribbons and model (see Methods)

Parameter	Parallel pair			Non-H-bonded pair			H-bonded pair		
	β-Sheets	β-Ribbons	Model	β-Sheets	β-Ribbons	Model	β-Sheets	β-Ribbons	Model
Sheet twist (deg.)	17 ± 7	23 ± 9	28 ± 8	15 ± 10	25 ± 16	18 ± 22	8 ± 8	20 ± 10	16 ± 18
Shear (Å)	0.1 ± 0.2	0.2 ± 0.3	0.2 ± 0.1	0.9 ± 0.2	0.8 ± 0.2	0.9 ± 0.1	0.6 ± 0.2	0.5 ± 0.2	0.4 ± 0.1
$d(C^{\beta} \cdots C^{\beta})$ (Å)	4.9 ± 0.4	5.1 ± 0.6	5.4 ± 0.3	5.2 ± 0.6	5.4 ± 0.6	4.7 ± 0.8	4.7 ± 0.5	5.1 ± 0.6	6.1 ± 0.5
$d(C^{\alpha} \cdots C^{\alpha})$ (Å)	4.8 ± 0.2	4.9 ± 0.2	5.1 ± 0.1	4.5 ± 0.2	4.5 ± 0.2	4.4 ± 0.2	5.2 ± 0.2	5.3 ± 0.2	5.7 ± 0.1
$d(O \cdots O)$ (Å)	3.7 ± 0.2	3.7 ± 0.2	3.8 ± 0.2	4.0 ± 0.3	3.9 ± 0.2	4.0 ± 0.2	3.6 ± 0.2	3.5 ± 0.2	3.4 ± 0.2
$d(H \cdots H)$ (Å)	3.8 ± 0.3	3.8 ± 0.2	3.9 ± 0.2	5.2 ± 0.5	4.8 ± 0.6	5.0 ± 0.5	2.8 ± 0.2	2.8 ± 0.2	3.1 ± 0.1
$d(H \cdots H^{\alpha})$ or $d(H^{\alpha} \cdots H^{\alpha})$ (Å)[a]	2.8 ± 0.2	2.7 ± 0.3	2.9 ± 0.1	2.4 ± 0.2	2.4 ± 0.2	2.4 ± 0.2	7.4 ± 0.2	7.4 ± 0.1	7.8 ± 0.1

[a] $d(H \cdots H^{\alpha})$ refers to the inter-strand hydrogen atom to hydrogen atom distance in the parallel pairs; $d(H^{\alpha} \cdots H^{\alpha})$ refers to the hydrogen atom to hydrogen atom distance in the antiparallel pairs.

and flexibility of the β-ribbons compared to the β-sheet.[22] The utility of the sheet twist is that we have measured significant correlations relating to the sheet twist (see the next section).

Correlations

We have measured a range of parameters of the inter-strand pairs in both the β-sheets and β-ribbons (some of the parameters are shown in Table 1). We have focused on correlations that relate inter-strand parameters with the φ-ψ angles (Table 2). These correlations are dominated by correlations of the non-H-bonded pairs. In particular, there is a correlation of sheet twist to φ in the non-H-bonded pairs in both the antiparallel β-ribbon (Figure 4(b)) and antiparallel β-sheet (Figure 4(d)). However, it is surprising to find that there is no correlation of sheet twist to ψ in both antiparallel β-ribbons (Figure 4(e)) and antiparallel β-sheets (Figure 4(g)). Furthermore, no significant correlation of sheet twist to the φ-ψ angles was found in the H-bonded pair or the parallel pair (Table 2).

We also observed a significant correlation of the sheet twist of the H-bonded pair to the sheet twist of the non-H-bonded pair in both the antiparallel β-ribbons (Figure 4(h)) and antiparallel β-sheets (Figure 4(j)). This correlation indicates that there is a significant coupling of the H-bonded pair to the neighbouring non-H-bonded pairs. Finally, we found correlations of φ to ψ in the H-bonded pair of the antiparallel β-ribbon (Figure 5(f)) and the narrow residue of the parallel β-ribbon (Figure 5(n)). Reproducing the correlations between the intra-strand parameters would be a sensitive test for the correct coupling between strands in a β-sheet.

Table 2. Significant correlations (>0.7) in inter-strand pairs observed between inter-strand parameters and other inter-strand parameters, and between inter-strand parameters and the φ-ψ angles

Correlation	Value
A. *Parallel β-ribbon pair*	
$d(H \cdots H^{\alpha})$ *versus* ψ_w	−0.70
Sheet twist *versus* sheet twist_{C-}	0.71
B. *Parallel β-sheet pair*	None
C. *Antiparallel β-ribbon H-bonded pair*	None
D. *Antiparallel β-ribbon non-H-bonded pair*	
Sheet twist *versus* φ	0.83
Sheet twist_{nHb} *versus* sheet twist_{Hb}	0.82
$d(H \cdots H)$ *versus* φ	−0.90
$\angle OH^{\alpha}\text{-}H^{\alpha}C^{\alpha}C^{a}$ *versus* ψ	−0.83
E. *Antiparallel β-sheet H-bonded pair*	None
F. *Antiparallel β-sheet non-H-bonded pair*	
Sheet twist *versus* φ	0.74
Sheet twist_{nHb} *versus* sheet twist_{Hb}	0.74
$d(H \cdots H)$ *versus* φ	−0.82
$\angle OH^{\alpha}\text{-}H^{\alpha}C^{\alpha}C^{a}$ *versus* ψ	−0.88

[a] $\angle OH^{\alpha}\text{-}H^{\alpha}C^{\alpha}C$ is the angle made by the $O \cdots H^{\alpha}$ vector of the bifurcated H-bond with the plane defined by the H^{α}, $C^{\alpha}C$ atoms.

The bifurcated hydrogen bond

There have been various studies that have reported the existence of a $C^{\alpha}H^{\alpha} \cdots O$ weak hydrogen bond in both the parallel and antiparallel β-sheets.[13,23] Consequently, we have measured the inter-atomic distance between the O and H^{α} atoms of the putative $C^{\alpha}H^{\alpha} \cdots O$ weak hydrogen bond and find that $d(O \cdots H^{\alpha}) = 2.5(\pm 0.2)$ Å in all β-structures. Observing the same value of $d(O \cdots H^{\alpha})$ in different structures is indicative of an interaction between the O and H^{α} atoms, and the observed values are consistent with the inter-atomic $O \cdots H$ distance of the $C\text{-}H \cdots O$ weak H-bond reported in a wide variety of different chemical systems.[12]

The formation of the $C^{\alpha}H^{\alpha} \cdots O$ H-bond combines with the $C{=}O \cdots H\text{-}N$ H-bond to form a bifurcated H-bond, where the carbonyl O atom on one strand forms a H-bond with both the amide H and the aliphatic H^{α} atom on the other strand (Figure 2(c)).[13] The antiparallel β-sheet must be sheared in order to incorporate the $C^{\alpha}H^{\alpha} \cdots O$ weak H-bond (Figure 1(b)). Once the bifurcated H-bond is included, the antiparallel β-sheet (Figure 1(b)) looks remarkably like the parallel β-sheet (Figure 1(c)).

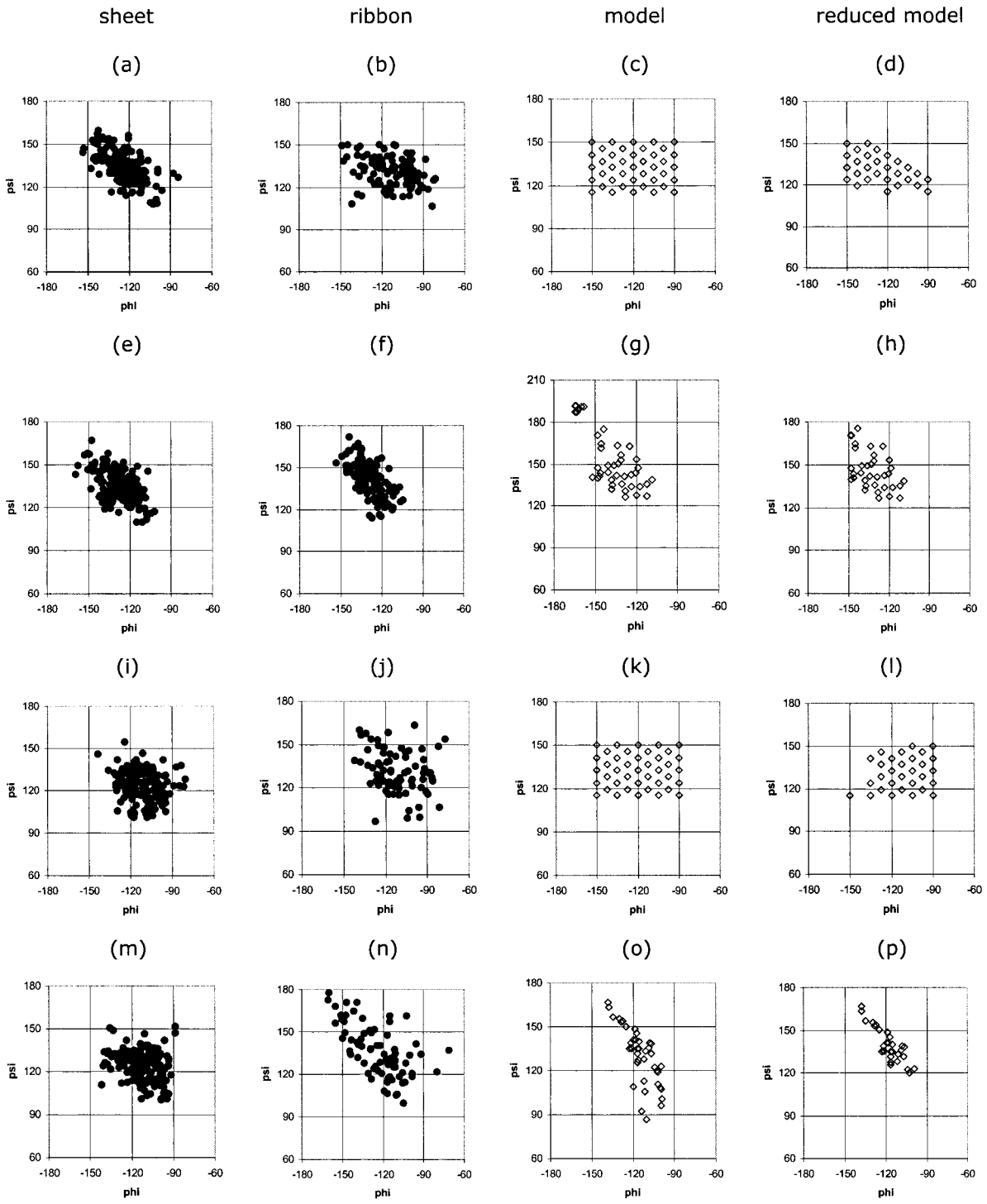

Figure 5. ϕ-ψ plots. Antiparallel non-H-bonded pair residue in: (a) β-sheet, slope −0.53, correlation coefficient (corr) −0.61; (b) β-ribbon, slope −0.20, corr −0.20; (c) model; and (d) reduced model. Antiparallel H-bonded pair residues in: (e) β-sheet, slope −0.49, corr −0.53; (f) β-ribbon, slope −0.76, corr −0.63; (g) model, slope −0.85, corr −0.83; (h) reduced model, slope −0.40, corr −0.47. Parallel wide residue in: (i) β-sheet, slope −0.22, corr −0.27; (j) β-ribbon, slope −0.25, corr −0.27; (k) model; and (l) reduced model. Parallel narrow residue in: (m) β-sheet, slope −0.18, corr −0.20; (n) β-ribbon, slope −0.61, corr −0.60; (o) model; and (p) reduced model, slope −0.69, corr −0.83.

The Ramachandran plot

In our measurements of the Ramachandran plots, the observed β-sheet region is smaller than the traditional β-region (Figure 2(a)) which was first observed by Muñoz & Serrano.[10] However, our β-sheet region is different from the region defined by Muñoz & Serrano, where we have used a more stringent definition of the β-sheet and a higher-resolution limit for the protein structures.

The confined region of the Ramachandran plot is a measure of the constraints experienced by residues embedded in β-sheets. In order to define the range of φ-ψ in the Ramachandran plots, we have used the 5th-95th percentile band of the observed data points of φ-ψ.

In the antiparallel β-ribbons, the Ramachandran plot of the non-H-bonded pair residue (Figure 5(b)) is different from the Ramachandran plot of the H-bonded pair residue (Figure 5(f)). In the antiparallel β-sheets, in contrast, the Ramachandran plots of the non-H-bonded pairs (Figure 5(a)) and H-bonded pair (Figure 5(e)) are indistinguishable. The identical Ramachandran plots in the antiparallel β-sheets can be shown to be the intersection of the two antiparallel β-ribbon Ramachandran plots and significant correlations found in the antiparallel β-ribbons are found also in the antiparallel β-sheets (see Appendix). In antiparallel β-sheets, the two Ramachandran plots of H-bonded pairs and non-H-bonded pairs are similar, because every residue in a β-sheet belong to two different inter-strand pairs. A similar analysis also holds (see Appendix for details) for the parallel β-sheet (Figure 5(i) and (m)) and β-ribbon (Figure 5(j) and (n)). Essentially, the conformations of β-sheets can be understood as the intersection of the conformations of the different residue types in β-ribbons.

The φ-ψ dihedral angles parameterise various intra-strand inter-atomic distances. We have analysed the observed intra-strand distances for the β-ribbons (see Appendix for details) and have found evidence of novel inter-atomic interactions that constrain the φ-ψ angles to the observed range of values.

First, the intra-strand distance $d(O\cdots H^{\alpha})$ of all β-residues is restricted to values of 2.4(±0.1) Å (Figure 6(a)-(d); Table 3), which corresponds to a non-bonded $O\cdots H^{\alpha}$, polar interaction (see Appendix for details). As $d(O\cdots H^{\alpha})$ is parameterised by φ, the formation of the non-bonded polar interaction restricts φ to values of $-150^{\circ} < \phi < -90^{\circ}$. Second, the intra-strand $d(H\cdots H^{\alpha})$ distances of 2.3(±0.1) Å facing the inside interface of both the parallel β-ribbons (Figure 6(g)) and antiparallel β-ribbons (Figure 6(e)) appear to be in steric contact. As hydrogen atoms do not attract each other electrostatically, this steric interaction must be forced by another interaction. This is satisfied by the inter-strand bifurcated H-bond (Figure 2(c)). As $d(H\cdots H^{\alpha})$ parameterises ψ, the resultant values of $d(H\cdots H^{\alpha}) = 2.3(\pm 0.1)$ Å restricts ψ to the range $90^{\circ} < \psi < 150^{\circ}$. The observed values of ψ are found within this range.

Third, although the bifurcated H-bonds restrict ψ to $90^{\circ} < \psi < 150^{\circ}$, the observed values of ψ in all β-residues are found in the upper half of this region (Figure 6(i)-(l)). We take the lower limit as $\psi > 116^{\circ}$, where this limit corresponds to the 5th percentile band threshold for the non-H-bonded pair residues. This limit corresponds to the lower limit of intra-strand $O\cdots C^{\beta}$ distance of $d(O\cdots C^{\beta}) < 2.9$ Å. As the typical $O\cdots C^{\beta}$ van der Waals radius is 3.15 Å, we interpret the observed limit as an intra-strand steric clash between the O and C^{β} atoms, which forces $\psi > 116^{\circ}$. However, the steric clash between the O and C^{β} atoms does not seem to hold for residues that are not part of β-sheets. In the $d(O\cdots C^{\beta})$ *versus* ψ distributions for all residues (Figure 7), there is a drop in density of data points in the right arm for $d(O\cdots C^{\beta}) < 2.9$ Å corresponding to the $O\cdots C^{\beta}$ steric clash. Nevertheless, there still remain a significant number of points for $d(O\cdots C^{\beta}) < 2.9$ Å. For these points, some other interaction must compensate for the unfavourable $O\cdots C^{\beta}$ interaction. There appear to be no such compensating interactions in β-structures and, thus, the van der Waals $O\cdots C^{\beta}$ steric clash restricts the range of ψ.

These interactions can be used to define the allowed region of the Ramachandran plot for residues in the antiparallel β-ribbon non-H-bonded pair and the parallel β-ribbon wide residue. The φ angle is restricted to $-150 < \phi < -90^{\circ}$ by the formation of the intra-strand $O\cdots H^{\alpha}$ non-bonded polar interaction. Two effects result in restrictions of ψ. First, the bifurcated inter-strand hydrogen bond restricts $d(H\cdots H^{\alpha})$ to 2.3(±0.1) Å and thus $90^{\circ} < \psi < 150^{\circ}$. This is symmetric to the restriction on φ. More significantly, the $O\cdots C^{\beta}$ steric clash further restricts ψ to $\psi > 116^{\circ}$, thus restricting the Ramachandran region to $116^{\circ} < \psi < 150^{\circ}$. The resulting region of the Ramachandran plot is $(-150^{\circ} < \phi < -90^{\circ};\ 116^{\circ} < \psi < 150^{\circ})$, which is asymmetric with respect to the diagonal (Figure 5(c) and (k)). This allowed region matches of the observed non-H-bonded pair Ramachandran plot (Figure 5(b)). Although the mechanisms that constrain the allowed region of the Ramachandran plot, also constrain the parallel β-ribbon wide residue, the allowed region (Figure 5(k); $-150^{\circ} < \phi < -90^{\circ}$) is noticeably larger in φ than the observed region of the wide residue (Figure 5(j); $-138^{\circ} < \phi < -87^{\circ}$). This needs to be accounted for. We also need to account for the correlated φ-ψ plots observed in the H-bonded pair of the antiparallel β-ribbon (Figure 5(f)) and in the narrow residue of the parallel β-ribbon (Figure 5(n)).

Modelling the antiparallel β-ribbon

To understand the origin of the observed sheet twist and shear of the antiparallel β-ribbon, we modelled the antiparallel β-ribbon using a representation of inter-strand interactions consisting of partial charge electrostatics and distance constraints, where the covalent bond lengths and angles were fixed to standard values. We modelled the antiparallel β-ribbon as an H-bonded pair coupled to a non-H-bonded pair, where we parameterised the φ-ψ angles of the non-H-bonded pair residues with values taken only from the allowed region of the Ramachandran plot (see the previous section). For each value of φ-ψ of the non-H-bonded pair, we minimised the inter-atomic potentials by allowing the translational and rotational

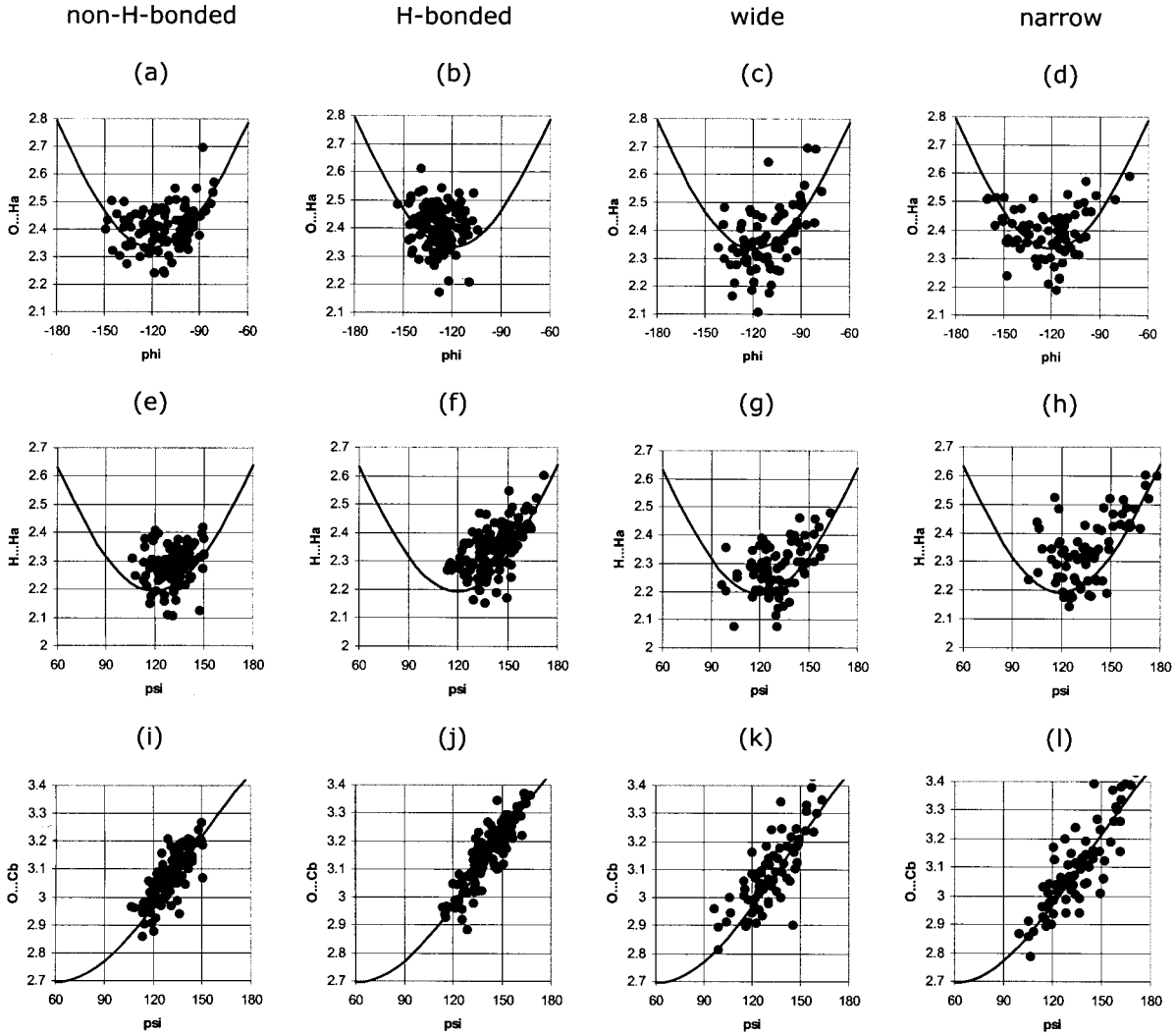

Figure 6. Intra-strand distances and ϕ-ψ angles in β-ribbons. $d(O\cdots H^{\alpha})$ *versus* ϕ in: (a) non-H-bonded pair residue, inner interface; (b) H-bonded pair residue, outer interface; (c) wide residue, inner interface; and (d) narrow residue, outer interface. $d(H\cdots H^{\alpha})$ *versus* ψ in: (e) non-H-bonded pair residue, inner interface; (f) H-bonded pair residue, outer interface; (g) wide residue, inner interface; and (h) narrow residue, outer interface. $d(O\cdots C^{\beta})$ *versus* ψ in: (i) non-H-bonded pair residue; (j) H-bonded pair residue; (k) wide residue; and (1) narrow residue.

degrees of freedom between the two strands and the ϕ-ψ angles of the residues to vary. This produced a unique minimum energy conformation of the coupled H-bonded and non-H-bonded pair (see Methods). As we sampled over the allowed region of the ϕ-ψ plot for the non-H-bonded pair, the model generated the set of allowed conformations of the coupled H-bonded and non-H-bonded pair. Distributions of sheet twist and shear were generated from the ensemble of allowed conformations of the model.

Table 3. Range of intra-strand inter-atomic distances that are parameterised by ϕ for the range $-150^{\circ} < \phi < -90^{\circ}$ (see Figure 2(b))

Intra-strand distance	Range (Å)	van der Waals contact radii (Å)
$d(O_{i-1}\cdots C^{\beta,i})$	3.4-4.2	3.05
$d(O_{i-1}\cdots H^{\alpha,i})$	2.3-2.5	2.57
$d(H_i\cdots C^{\beta,i})$	5.4-6.2	2.65
$d(H_i\cdots H^{\alpha,i})$	4.8-5.0	2.17

The subscript/superscript on the atoms refers to whether an atom belongs to the backbone component of residue *i*, or to the backbone component of residue $i-1$, the neighbouring residue along the strand in the N-terminal direction. Only the O_{i-1} and $H^{\alpha,i}$ atoms are in contact for the given range of ϕ.

There have been two previous interactions that have been proposed to explain the shear. The first interaction is the interaction between inter-strand CO dipoles (Figure 1(d)).[4] The second interaction is essentially an inter-strand O···O repulsion in the H-bonded pair, which we have modelled as an electrostatic interaction between the CO···NH groups in the H-bonded pair (Figure 1(d)).[18] In addition, as inter-strand $C^{\alpha}H^{\alpha}\cdots O$ hydrogen bonds are always found in β-sheets, we have considered a model consisting of just $C^{\alpha}H^{\alpha}\cdots$OH-

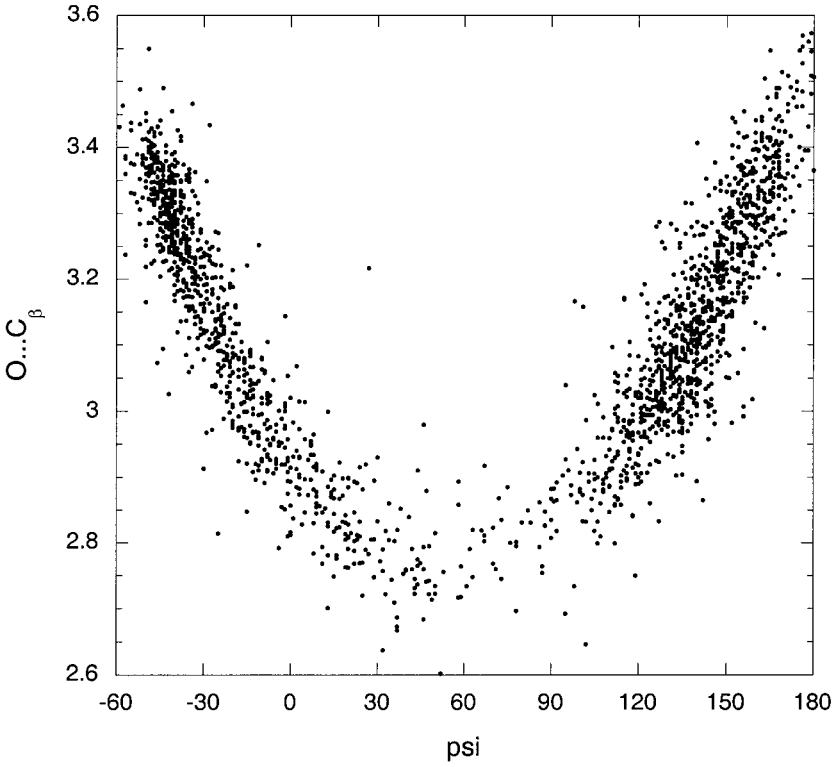

Figure 7. $d(O\cdots C^{\beta})$ *versus* ψ for all residues taken from structures with resolution better than 1.3 Å. There is a drop in density of points for $d(O\cdots C^{\beta}) < 2.9$ Å, especially for the right branch of the curve.

bonds. In all three cases, the canonical inter-strand CO···NH H-bond interaction is required to hold the strands together in the β-ribbon. Although a full partial charge model of the antiparallel β-ribbon would include all three interactions, we have modelled each of the three interactions separately. This allows us to identify the specific inter-strand interaction responsible for the observed correlations of twist and shear (see Methods).

The CO dipole interaction produced values of non-H-bonded shear that match the observed values to within 0.1 Å and the inter-strand $O\cdots H^{\alpha}$ distance also match to within 0.1 Å (Table 4). However, the H-bonded pair shear match only within 0.3 Å. The interacting CO···NH groups produced conformations that did not reproduce values of shear that match the observed values (Table 4). The $C^{\alpha}H^{\alpha}\cdots O$ weak H-bond interaction produced the best values of shear, which match the observed values to within 0.1 Å (Table 4). As the $C^{\alpha}H^{\alpha}\cdots O$ weak H-bond is a direct inter-atomic interaction, it is a more plausible interaction than the other two interactions, which are long-range electrostatic interactions.

In the next few sections, we show that the model of the bifurcated H-bond interaction reproduced the observed correlations in the antiparallel and parallel β-ribbons. These correlations were not reproduced by the model using the inter-strand CO dipole interaction or the inter-strand O···O interaction (data not shown).

The bifurcated H-bond in the anti parallel β-ribbon

The model using the bifurcated H-bond reproduced all the significant correlations (second column in Figures 4 and 8) that were observed in the antiparallel β-ribbons (first column in Figures 4 and 8). In particular, the model produced the bias of the right-hand twist as the distribution of the sheet twist of the H-bonded pair *versus* the non-H-bonded pair (Figure 4(i)) matches the observed distribution (Figure 4(h)). The sheet twist distributions lies mostly in the upper-right quadrant of the graph, corresponding to the right-hand twist in the H-bonded and non-H-bonded pairs. The model produced values that match the observed values to

Table 4. Parameters of different models of the antiparallel β-ribbon compared with data

Parameters	Antiparallel β-ribbon data (Å)	Bifurcated H-bond (Å)	CO···CO dipole-dipole interaction (Å)	Interacting CO···HN groups (Å)
$d(O\cdots H^{\alpha})$	2.5 ± 0.2	2.5 ± 0.0	2.6 ± 0.1	3.2 ± 0.1
Hb shear	0.5 ± 0.2	0.4 ± 0.1	0.2 ± 0.0	-0.5 ± 0.1
nHb shear	0.8 ± 0.2	0.9 ± 0.2	0.7 ± 0.1	0.4 ± 0.1

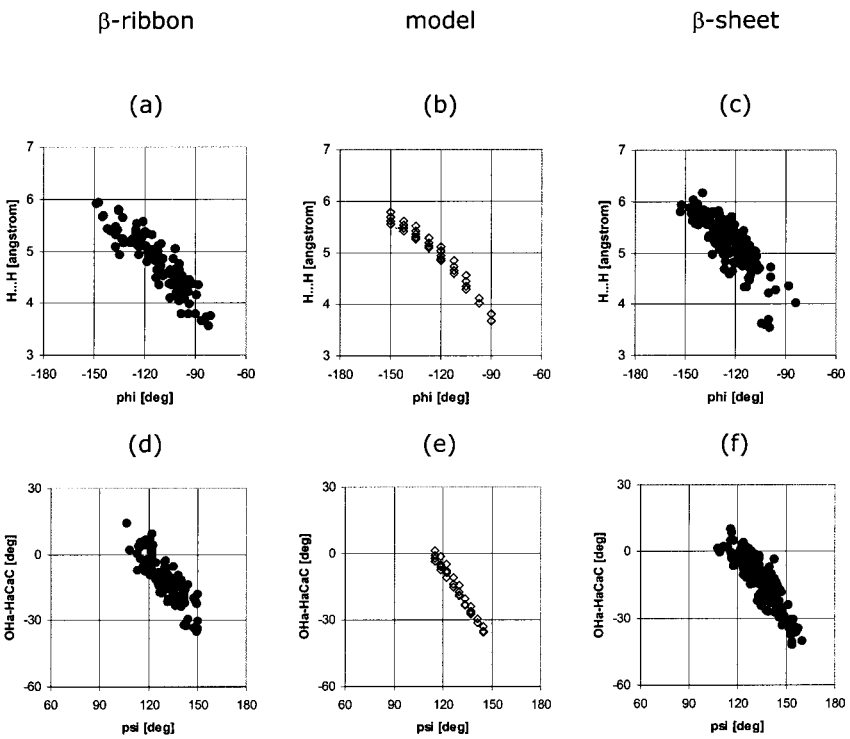

Figure 8. Significant correlations in the antiparallel non-H-bonded pair. Inter-strand $d(H\cdots H)$ *versus* ϕ in: (a) β-ribbon, slope −0.031, correlation coefficient (corr) −0.90; (b) model, slope −0.027, corr −0.97; and (c) β-sheets, slope −0.031, corr −0.82, <OH^{α}-$H^{\alpha}C^{\alpha}C$ is the angle made by the $O\cdots H^{\alpha}$ vector of the bifurcated hydrogen bond with the plane defined by the H^{α}, C^{α} C atoms. <OH^{α}-$H^{\alpha}C^{\alpha}C$ *versus* ψ in: (a) β-ribbons, slope −0.83, corr −0.84; (b) model, slope −1.17, corr −0.99; and (c) β-sheets, slope −0.92, corr −0.88.

within 0.1 Å for many different parameters of the antiparallel β-ribbon (Table 1).

The model generated a correlated H-bonded pair Ramachandran plot (Figure 5(g)) that has approximately the same shape and slope as the observed plot (Figure 5(f)). However, the model ϕ-ψ plot extends out much further than the observed plot ($\phi < -146^{\circ}$). If we make the assumption that the intra-strand $O\cdots H^{\alpha}$ non-bonded polar interaction forms also in the H-bonded pair, then we can eliminate from the ensemble of allowed conformation of the model any conformation where the $O\cdots H^{\alpha}$ non-bonded polar interaction is not formed ($\phi < -150^{\circ}$) in the H-bonded pair. This reduces the Ramachandran plot of the H-bonded pair generated by the model (Figure 5(h)) that better matches the observed distribution (Figure 5(f)). As an added bonus, the non-H-bonded pair ϕ-ψ distribution is reduced to an ellipsoidal distribution (Figure 5(d)) that better matches the observed distribution (Figure 5(b)). Thus, the correlated ϕ-ψ plot in the H-bonded pair is simply due to coupling an H-bonded pair to a non-H-bonded pair.

Analysing the sheet twist using the model

Given a reliable model of the antiparallel β-ribbon, we can explore the relationship between the Ramachandran plot and the sheet twist. We recalculated the model using a different region in ϕ-ψ of ($-150^{\circ} < \phi < -90^{\circ}$; $90^{\circ} < \psi < 150^{\circ}$), which ignores the intra-strand $O\cdots C^{\beta}$ steric clash ($\psi < 116^{\circ}$). This region is symmetric with respect to ϕ and ψ, and is not biased towards the upper region of the main diagonal of the Ramachandran plot. The resultant sheet twist is $5(\pm 33)^{\circ}$, which is not biased towards the positive right-hand twist, suggesting that the right-hand sheet twist depends on the $O\cdots C^{\beta}$ steric clash to force the allowed region above the main diagonal of the Ramachandran plot.

Using the symmetric ϕ-ψ region, the model produced a correlation of sheet twist to ϕ of −0.79 and a correlation of sheet twist to ψ of 0.70. As the previous model produced a sharp correlation of −0.96 for sheet twist *versus* ϕ and a poor correlation of 0.52 for sheet twist *versus* ψ, the difference between ϕ and ψ has disappeared. By using the symmetric distribution, we have lost both the correlation of sheet twist to ϕ and the right-hand twist. We conclude that the correlation of sheet twist to ϕ is simply due to the allowed region being wider in ϕ than ψ (Figure 5(c)).

Modelling the parallel pair

We modelled the parallel pair in order to understand the correlation in the narrow residue ϕ-ψ plot and to see if a model of the bifurcated hydrogen bonds can reproduce the observed conformations of the parallel pair, including the positive right-hand sheet twist (Table 1). We modelled a parallel pair (Figure 1(e)); we fixed the covalent bond lengths and angles to standard values. We modelled the two bifurcated H-bonds in the parallel pair (Figure 1(e)) with the same inter-atomic potential as in the antiparallel model. We had to apply an extra constraint to the parallel pair in order to model the restrictions correctly, due to the neighbouring pairs in a parallel β-ribbon (see

Methods). The variables in the model consist of the translational and rotational degrees of freedom between the two strands and the ϕ-ψ angles of the residues. For each value of ϕ-ψ in the wide residue, minimising the inter-atomic potentials generated a unique minimum energy conformation of the parallel pair (see Methods). As we sampled over the allowed region of the ϕ-ψ plot for the wide residue, the model generated the set of allowed conformations of the parallel pairs.

From the set of allowed conformations of the parallel pair, we extracted the narrow residue ϕ-ψ plot (Figure 5(o)). The top half of the distribution approximately matches the observed correlation (Figure 5(n)), whereas the bottom half does not. However, the values of ψ found in the bottom half correspond to an intra-strand $O\cdots C^{\beta}$ steric clash. From the set of allowed conformations of the parallel pair, we eliminated conformations where there was an $O\cdots C^{\beta}$ steric clash in the narrow residue ($\psi < 116^{\circ}$). The resultant reduced ϕ-ψ plot in the narrow residue (Figure 5(p)) better matches the observed plot (Figure 5(n)). Eliminating such conformations also reduces the model wide residue distribution (Figure 5(l)), which better matches the observed distribution (Figure 5(j)). The combination of the bifurcated H-bonds and the constraints of neighbouring parallel pairs induce the observed correlated ϕ-ψ plot in the narrow residue.

The model produced values of the inter-strand parameters that match the observed values (Table 1). The parameters match to within 0.2 Å for distances involving main-chain atoms and within 0.4 Å for the side-chain $C^{\beta}\cdots C^{\beta}$ distance. The model of the parallel pair produced positive right-handed values of sheet twist with an average value that matched the observed values to within 5° with a comparable standard deviation.

The tightly packed β-sheet interface

If we consider the interactions in the interface between the β-strands ($CO\cdots NH$ and $C^{\alpha}H^{\alpha}\cdots O$ H-bonds; intra-strand $O\cdots H^{\alpha}$ interactions and $H\cdots H^{\alpha}$ steric contacts) the interface of both the antiparallel β-ribbon (Figure 9(a)) and parallel β-ribbon (Figure 9(b)) are tightly packed. The main difference between the antiparallel and parallel β-ribbon interface is that an inter-strand $H^{\alpha}\cdots H^{\alpha}$ steric contact is found in the antiparallel β-ribbon interface (2.4(±0.2) Å), which is not found in the analogous $H\cdots H^{\alpha}$ distance in the parallel β-ribbon interface (2.8(±0.2) Å).

Discussion

The weak $C^{\alpha}H^{\alpha}\cdots O$ H-bond

Although there is already an extensive literature demonstrating the existence of the $CH\cdots O$ weak H-bond in a wide class of chemical systems,[12,13,24,25] the existence of the $C^{\alpha}H^{\alpha}\cdots O$ weak H-bond in proteins is still a matter of debate.[31] However, we have shown that the $C^{\alpha}H^{\alpha}\cdots O$ weak H-bond is needed to form the bifurcated H-bonds in order to constrain ψ and to shear the antiparallel β-sheet and antiparallel β-ribbon. The study of an atomic force-field representation of the $C^{\alpha}H^{\alpha}\cdots O$ weak H-bond will be an important next step in the study of protein structure.

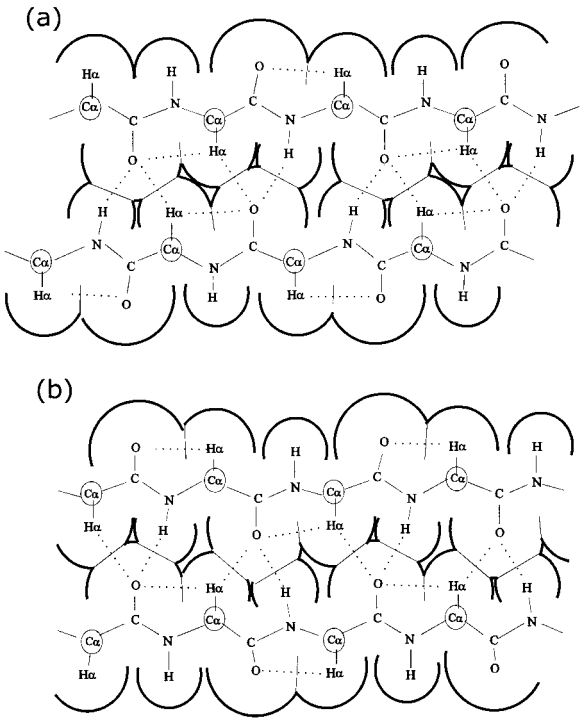

Figure 9. Schematic of the tight packing in the β-ribbon interface in (a) the antiparallel β-ribbon and (b) the parallel β-ribbon. There is an extra $H^{\alpha}\cdots H^{\alpha}$ steric contact in the non-H-bonded pair of the antiparallel β-ribbon that is not found in the parallel β-ribbon.

The origin of the right-hand twist

We have found that the bifurcated H-bonds, in both the antiparallel and parallel β-ribbon, couple the sheet twist to the ϕ-ψ angles where the range of sheet twist depends on the location of the allowed region of the Ramachandran plot. In previous studies, it was assumed that there was a coupling between the twisting of the β-sheet and the ϕ-ψ angles.[14–18] In this study, we have been able to measure this coupling directly (Figure 4).

The allowed region of the Ramachandran plot for both the antiparallel non-H-bonded pair residue and the parallel wide residue, is determined by: (a) the intra-strand $O\cdots H^{\alpha}$ non-bonded polar interaction; (b) the inter-strand bifurcated H-bonds; and (c) the intra-strand $O\cdots C^{\beta}$ steric clash. Of the three contributing factors, formation of the $O\cdots H^{\alpha}$ interaction and the bifurcated H-bond stabilises the region in ϕ-ψ of ($-150^{\circ} < \phi < -90^{\circ}$;

$90° < \psi < 150°$). This region is symmetric around the diagonal of the Ramachandran plot and will not produce a bias for the right-hand twist. It is the $O\cdots C^{\beta}$ steric clash that shifts the allowed region of the Ramachandran plot to ($-150° < \phi < -90°$; $116° < \psi < 150°$). This region is above the diagonal of the Ramachandran plot and corresponds to twisted β-strands. Coupling such β-strands with bifurcated H-bonds will induce a right-hand sheet twist.

The $O\cdots C^{\beta}$ steric interaction

The role of the $O\cdots C^{\beta}$ steric clash in the right-hand twist was first suggested by Yang & Honig,[16] who identified a favourable $O\cdots C^{\beta}$ steric contact in models of right-hand twisted antiparallel β-sheets but not in left-hand twisted β-sheets. However, Wang and co-workers[19] found that intra-strand $O\cdots C^{\beta}$ van der Waals contacts are easily broken in molecular dynamics simulations of β-strands. Consequently, they argued that inter-strand interactions must stabilise the right-hand twist and that the $O\cdots C^{\beta}$ steric clash cannot be the driving force of the right-hand twist. Our mechanism for the right-hand twist satisfies these objections. We have identified an inter-strand interaction, the bifurcated H-bond that stabilises part of the allowed β-sheet region of the Ramachandran plot of ($90° < \psi < 150°$). However, only if the intra-strand $O\cdots H^{\alpha}$ non-bonded polar interaction also stabilises the region ($-150° < \phi < -90°$), can the $O\cdots C^{\beta}$ steric clash induce a right-hand twist. We have found that fewer residues are found with $d(O\cdots C^{\beta}) < 2.9$ Å in high-resolution structures and these residues (that are not in β-structures) are presumably stabilised by other interactions that compensate for the unfavourable $O\cdots C^{\beta}$ steric clash.

The β-sheet region of the Ramachandran plot

By coupling an H-bonded pair to a non-H-bonded pair with bifurcated H-bonds, we can reproduce the correlated Ramachandran plot of the H-bonded pair residues in antiparallel β-ribbons. Similarly, coupling a narrow residue to a wide residue will account for the correlated Ramachandran plot of the narrow residue in parallel β-ribbons. The observed conformations of β-sheets can be shown to be the intersections of the conformations of the different residue types in β-ribbons.

Methods

Data set

We used DSSP[9] to identify β-sheet and β-ribbon residues. For β-ribbons, we have used the non-redundant representative list of protein structures from the PDB[26] that include positions for all hydrogen atoms and where the resolution is better than 1.7 Å.[31] Unfortunately, the sample size of this data set was inadequate for interior β-sheet residues. For β-sheets, we have used the 1996 list of non-redundant representative protein structures[27] in which no pair of chains in the set exceeds 25 % sequence identity. As we have restricted the sample size severely by using only interior β-sheet residues, we use a more generous resolution limit, better than 2.0 Å, to generate a sample size for the data set comparable with the β-ribbon data set. As the positions of projected hydrogen atoms of high-resolution structures have been shown to be reliable,[31] we projected the positions of missing amide hydrogen atoms from the backbone using the standard geometry of the peptide unit,[28] and we projected the position of missing H^{α} atoms using tetrahedral bonding at the C^{α} atom.

We excluded glycine and proline residues, and β-bulges from the analysis. We considered only interior residues from β-sheets. For β-sheets, there were 200 antiparallel H-bonded pairs, 175 antiparallel non-H-bonded pairs and 172 parallel pairs. For β-ribbons, there were 134 H-bonded pairs, 106 non-H-bonded pairs and 80 parallel pairs.

Definition of the backbone direction vector

We define the backbone direction vector of a residue as the vector joining the point equidistant from the N and C atoms of the two peptide units that form the backbone of the residue (see the peptide unit in Figure 3(a)).

Definition of shear

In the antiparallel H-bonded pair and the non-H-bonded pair, we define the shear as the displacement of the C^{α} atom of residue 1 along the backbone direction $\mathbf{b_1}$-$\mathbf{b_2}$ from the perpendicular projected from the C^{α} atom of residue 2 (Figure 3(a)). The C^{α} atom is used, since it is the stereo-chemical centre of the residue. We take the backbone direction of a pair of inter-strand residues as the difference of the backbone vectors of the respective residues, $\mathbf{b_1}$ and $\mathbf{b_2}$, where $\mathbf{b_1}$ is chosen arbitrarily. The backbone direction points in the N to C-terminal direction of residue 1. Due to the dyad symmetry of the antiparallel pairs, the defined shear can take on positive and negative values where the sign and magnitude of shear is invariant with respect to the choice of residue 1 and residue 2.

We define the backbone direction vector of the parallel inter-strand pair as the sum of the backbone vectors of the wide and narrow residue, $\mathbf{b_w}$ and $\mathbf{b_n}$. Parallel shear is defined as the displacement of the wide residue $C^{\alpha,W}$ atom along the backbone direction with respect to the $C^{\alpha,n}$ atom of the narrow residue in the backbone direction, where both C^{α} positions are determined by drawing a perpendicular from the backbone direction. Shear in the parallel pair can take on positive and negative values, which are defined uniquely.

Definition of sheet twist

We define the sheet twist, in both the antiparallel H-bonded pair and the non-H-bonded pair as the acute angle between the backbone vectors, $\mathbf{b_1}$ and $\mathbf{b_2}$, of a pair of inter-strand neighbouring residues (Figure 4(a)). If the inter-strand pair is right-hand twisted, then the cross product $\mathbf{b_1} \times \mathbf{b_2}$ will be pointing roughly in the direction of $\mathbf{d_{21}}$, the vector from $C^{\alpha,2}$ to $C^{\alpha,1}$. Otherwise, the inter-strand pair is left-hand twisted. Consequently, we have defined the sign of the sheet twist as the sign of the scalar product between $\mathbf{b_1} \times \mathbf{b_2}$ and $\mathbf{d_{21}}$ ($(\mathbf{b_1} \times \mathbf{b_2})\cdot\mathbf{d_{21}}$). Since both $\mathbf{b_1} \times \mathbf{b_2}$ and $\mathbf{d_{21}}$ change signs if the labels 1

and 2 are reversed, this definition of sheet twist is invariant with respect to the choice of residue 1.

The parallel sheet twist is defined as the acute angle between the backbone vectors, $\mathbf{b_n}$ and $\mathbf{b_w}$, of a pair of inter-strand neighbouring residues. The sign of the sheet twist is taken to be the sign of the scalar product between the vectors, $\mathbf{b_n} \times \mathbf{b_w}$ and $\mathbf{d_{wn}}$ the vector joining $C^{\alpha,W}$ to $C^{\alpha,n}$ ($(\mathbf{b_n} \times \mathbf{b_w}) \cdot \mathbf{d_{wn}}$). If the sign is negative, the sheet twist is positive and right-handed; otherwise, the sheet twist is negative and left-handed.

Modelling the β-sheet

In our model, we fixed the bond lengths and angles of the backbone to standard values.[28] Consequently, the only degrees of freedom in the backbone are the ϕ-ψ dihedral angles and intra-strand inter-atomic distances are parameterised only by the ϕ-ψ dihedral angles. We used alanine side-chains, as this represents the minimal side-chain. We use the Powell algorithm[29] to minimise the inter-atomic potentials between the two backbone fragments by varying the translational and rotational degrees of freedom between the residues of the inter-strand pairs and by varying any free ϕ-ψ angles.

Inter-strand inter-atomic potentials

As our models are concerned mainly with geometric properties, we have used a combination of distance constraints and partial charges to model the inter-atomic interactions. As we have kept our models fairly simple, the distance constraints are always satisfied where the distance constraint energies are zero at the minimum energy conformation. We have modelled the canonical CO···HN hydrogen bond with:
where we used a distance constraint to force $d(\mathrm{O}\cdots\mathrm{H})$ to

$$E_{\mathrm{CO\cdots HN}} = 331\left(\frac{q_{\mathrm{O}}q_{\mathrm{H}}}{r_{\mathrm{O\cdots H}}} + \frac{q_{\mathrm{C}}q_{\mathrm{H}}}{r_{\mathrm{C\cdots H}}} + \frac{q_{\mathrm{N}}q_{\mathrm{O}}}{r_{\mathrm{N\cdots O}}} + \frac{q_{\mathrm{C}}q_{\mathrm{N}}}{r_{\mathrm{C\cdots N}}}\right) + (r_{\mathrm{O\cdots H}} - 2.0\ \text{Å})^2 \quad (1)$$

take on the observed value of 2.0 Å and we use electrostatics to model the linearity properties of the CO···HN H-bond, where partial charge values taken from CHARMM[30] were used ($q_{\mathrm{c}} = 0.55\mathrm{e}$, $q_{\mathrm{H}} = 0.25\mathrm{e}$, $q_{\mathrm{N}} = -0.35\mathrm{e}$ and $q_{\mathrm{O}} = -0.55\mathrm{e}$). We used the distance constraint because we wanted to look at sub-sets of the interactions of the antiparallel β-ribbon where the model is unstable. The distance constraint is artificially stable and adequately simulates the van der Waals and partial interaction between the O and H atoms in the CO···HN hydrogen bond.

For the antiparallel β-ribbon, we examined three different inter-strand interactions. (1) We represented the inter-strand CO···CO dipole-dipole interaction as:

$$E_{\mathrm{CO\cdots C'O'}} = 331\left(\frac{q_{\mathrm{C}}q_{\mathrm{C'}}}{r_{\mathrm{C\cdots C'}}} + \frac{q_{\mathrm{O}}q_{\mathrm{O'}}}{r_{\mathrm{O\cdots O'}}} + \frac{q_{\mathrm{C}}q_{\mathrm{O'}}}{r_{\mathrm{C\cdots O'}}} + \frac{q_{\mathrm{O}}q_{\mathrm{C'}}}{r_{\mathrm{O\cdots C'}}}\right) \quad (2)$$

For the total interaction potential E_{total} of the CO···CO dipole-dipole interaction, we have considered only the interaction of CO dipoles, which will end up aligned:

$$E_{\mathrm{total}} = \sum_{i=1}^{3} E_{\mathrm{CO\cdots HN}}(i) + \sum_{i=1}^{3} E_{\mathrm{CO\cdots C'O'}}(i) \quad (3)$$

where the indices 1, 2, 3 represent the CO···CO dipole-dipole interactions in Figure 1(d) from left to right.

(2) For the interaction between the CO···HN group and the C′O′···H′N′ group, we considered only the inter-strand components where:

$$E_{\mathrm{int}} = 331\left(\frac{q_{\mathrm{N}}q_{\mathrm{N'}}}{r_{\mathrm{N\cdots N'}}} + \frac{q_{\mathrm{H}}q_{\mathrm{H'}}}{r_{\mathrm{H\cdots H'}}} + \frac{q_{\mathrm{N}}q_{\mathrm{H'}}}{r_{\mathrm{N\cdots H'}}} + \frac{q_{\mathrm{H}}q_{\mathrm{N'}}}{r_{\mathrm{H\cdots N'}}} + \frac{q_{\mathrm{C}}q_{\mathrm{C'}}}{r_{\mathrm{C\cdots C'}}} + \frac{q_{\mathrm{O}}q_{\mathrm{O'}}}{r_{\mathrm{O\cdots O'}}} + \frac{q_{\mathrm{C}}q_{\mathrm{O'}}}{r_{\mathrm{C\cdots O'}}} + \frac{q_{\mathrm{O}}q_{\mathrm{C'}}}{r_{\mathrm{O\cdots C'}}}\right) \quad (4)$$

In the case of the interacting CO···HN groups, we consider only the interaction between the CO···HN groups within the H-bonded pair and within the non-H-bonded pair, where the total inter-strand interaction potential is:

$$E_{\mathrm{total}} = \sum_{i=1}^{3} E_{\mathrm{CO\cdots HN}}(i) + E_{\mathrm{int}}(1,2) + E_{\mathrm{int}}(2,3) \quad (5)$$

(3) A bifurcated H-bond consists of a $C^{\alpha}H^{\alpha}\cdots O$ weak hydrogen bond and a CO···HN H-bond where the O atom is shared between the two H-bonds (Figure 2(c)). We have modelled the $C^{\alpha}H^{\alpha}\cdots O$ weak H-bond with a distance constraint:

$$E_{\mathrm{C\alpha H\alpha\cdots O}} = (r_{\mathrm{O\cdots H\alpha}} - 2.5\ \text{Å})^2 \quad (6)$$

We used a distance constraint because we could not generate realistic binding energies using van der Waals interactions and partial charge electrostatics, especially since CHARMM does not give a value for the partial charge of H^{α}. We have neglected the directional properties of the $C^{\alpha}H^{\alpha}\cdots O$ H-bond. However, this is relatively unimportant when the $C^{\alpha}H^{\alpha}\cdots O$ weak H-bond is part of a bifurcated H-bond. Consequently, the bifurcated H-bond interaction is:

$$E_{\mathrm{bif}} = E_{\mathrm{C\alpha H\alpha\cdots O}} + E_{\mathrm{CO\cdots HN}} \quad (7)$$

The resultant inter-strand interaction potential is:

$$E_{\mathrm{total}} = \sum_{i=1}^{3} E_{\mathrm{bif}}(i) \quad (8)$$

where the indices 1, 2, 3 represent the bifurcated H-bonds in Figure 1(d) from left to right.

Antiparallel β-ribbon model

Our model of the antiparallel β-ribbon consists of a non-H-bonded pair coupled to an H-bonded pair (Figure 1(d)). The backbone of the H-bonded pair has to be extended to include the H^{α} atom in order to model the outer bifurcated H-bonds of the H-bonded pair (leftmost bifurcated H-bond in Figure 1(d)). This extension of the backbone is parameterised by a ψ dihedral angle. Assuming dyad symmetry of the H-bonded pair, we parameterised this ψ angle with the same value as the ψ angle of the non-H-bonded pair (see Figure 1(d)). We must specify an inter-strand interaction E_{total} for the model. To construct the allowed conformations of the antiparallel pairs, we proceed as follows. (i) Assuming dyad symmetry, parameterise both residues of a non-H-bonded pair with a value of ϕ-ψ from the allowed distribution. (ii) Extend the backbone of the non-H-bonded pair residues to project out an H-bonded pair with arbi-

trary ϕ-ψ angles. (iii) Minimise E_{total} by varying the rotational and translational degrees of freedom between the two strands and the ϕ-ψ angles of the H-bonded pair simultaneously; this produces a conformation of the H-bonded pair coupled to the non-H-bonded pair. (iv) Repeat (ii)-(iii) for the other values of ϕ-ψ of the allowed distribution to generate the allowed set of conformations of the non-H-bonded pair and the H-bonded pair; and (v) from the set of allowed conformations, generate the ϕ-ψ distribution of the H-bonded pair residue, the range of the shear, and the correlations for comparison with the observations.

Parallel pair model

In order to model the parallel β-ribbon correctly, we need to take into account the restrictions due to neighbouring parallel pairs. Although we tried various ways of modelling two coupled parallel pairs, we found that the only way to produce a correlated ϕ-ψ plot in the narrow residue (Figure 5(n)) was to apply an artificial constraint to a single parallel pair.

This constraint can be understood by considering the twisting properties of a single parallel pair. A single parallel pair can adopt very twisted conformations consistent with the formation of hydrogen bonds. For some highly twisted conformations of the parallel pair, it is impossible for a neighbouring parallel pair in the C-terminal direction to form. One way to see whether the C-terminal neighbouring pair can form is to measure the $C^{\alpha}\cdots C^{\alpha}$ distance of the neighbouring pair: $d(C^{\alpha}\cdots C^{\alpha})_{,C-}$. As the observed range of $d(C^{\alpha}\cdots C^{\alpha})$ is 4.9(±0.2) Å, the C-terminal neighbouring pair cannot form unless $d(C^{\alpha}\cdots C^{\alpha})_{,C-}$ is within the range 4.7 Å to 5.1 Å.

A model of the parallel pair that is consistent with the requirement that neighbouring parallel pairs can form must produce values for both $d(C^{\alpha}\cdots C^{\alpha})$ and $d(C^{\alpha}\cdots C^{\alpha})_{,C-}$ in the range 4.7 Å to 5.1 Å. We found that the best way to model this was by artificially forcing $d(C^{\alpha}\cdots C^{\alpha})_{,C-}$ to be the same as $d(C^{\alpha}\cdots C^{\alpha})$ using:

$$E_{constrain} = (d(C^{\alpha}\cdots C^{\alpha}) - d(C^{\alpha}\cdots C^{\alpha})_{,C-})^2 \qquad (9)$$

The advantage of this constraint is that it does not contain any explicit distance parameter.

For the parallel β-ribbon, we modelled a single parallel pair (Figure 1(e)) in which two bifurcated H-bonds interact between the two strands and we applied a constraint due to neighbouring parallel pairs. Consequently, the inter-strand interaction potential is:

$$E_{total} = E_{bif}(1) + E_{bif}(2) + E_{constrain} \qquad (10)$$

The backbone of the narrow residue has to be extended to include the H^{α} atom in order to model the N-terminal bifurcated H-bond $E_{bif}(1)$ (left bifurcated H-bond in Figure 1(e)). This extension of the backbone is parameterised by a ψ angle, which we parameterise with the same value as the ψ angle of the wide residue (Figure 1(e)). To produce the correlations, we proceed as follows. (i) Parameterise the wide residue with a value of ϕ-ψ from the allowed ϕ-ψ distribution. (ii) Minimise E_{total} of the parallel subunit by varying the translational and rotational degrees of freedom and (ϕ_n, ψ_n); a unique conformation of the parallel pair is generated. (iii) Repeat (i)-(ii) for other values of ϕ-ψ of the wide residue from the allowed ϕ-ψ distribution to produce a set of allowed conformations of the parallel pair; and (iv) from the set of allowed conformations, generate the ϕ-ψ distribution of the narrow bonding residue and the range of the inter-strand parameters.

Acknowledgements

We thank Andrew Torda and Martin Zuckermann for many fruitful discussions during the course of this work. B.H. was a recipient of an Australian Postgraduate Award.

References

1. Pauling, L. & Corey, R. B. (1951). Configurations of polypeptide chains with favored orientations around single bonds: two new pleated sheets. *Proc. Natl Acad. Sci. USA,* **37**, 729-741.
2. Fraser, R. D. B. & MacRae, T. P. (1973). *Conformation in Fibrous Proteins*, pp. 218-246, Academic Press, New York and London.
3. Wouters, M. A. & Curmi, P. M. G. (1995). An analysis of side chain interactions and pair correlations within antiparallel β-sheets: the differences between backbone hydrogen-bonded and non-hydrogen-bonded residue pairs. *Proteins: Struct. Funct. Genet.* **22**, 119-131.
4. MacCallum, P. H., Poet, R. & Milner-White, E. J. (1995). Coulombic interactions between partially charged main-chain atoms not hydrogen-bonded to each other influence the conformations of α-helices and antiparallel β-sheet. A new method for analysing the forces between hydrogen bonding groups in proteins includes all the coulombic interactions. *J. Mol. Biol.* **248**, 361-373.
5. Artymiuk, P. J. & Blake, C. C. F. (1981). Refinement of human lysozyme at 1.5 Å resolution analysis of non-bonded and hydrogen-bond interactions. *J. Mol. Biol.* **152**, 737-762.
6. Stickle, D. F., Presta, L. G., Dill, K. A. & Rose, G. D. (1992). Hydrogen bonding in globular proteins. *J. Mol. Biol.* **226**, 1143-1159.
7. Ramachandran, G. N., Ramakrishnan, C. & Sasisekharan, V. (1963). Stereochemistry of polypeptide chain configurations. *J. Mol. Biol.* **7**, 95-99.
8. Ramachandran, G. N. & Sasisekharan, V. (1968). Conformation of polypeptides and proteins. *Advan. Protein Chem.* **23**, 284-438.
9. Kabsch, W. & Sander, C. (1983). Dictionary of protein secondary structure: pattern recognition of hydrogen-bonded and geometrical features. *Biopolymers,* **22**, 2577-2637.
10. Muñoz, V. & Serrano, L. (1994). Intrinsic secondary structure propensities of the amino acids, using statistical ϕ-ψ matrices: comparison with experimental scales. *Proteins: Struct. Funct. Genet.* **20**, 301-311.
11. Pauling, L. (1960). *The Nature of the Chemical Bond*, 3rd edit., p. 459, Cornell University Press, Ithaca, NY.
12. Taylor, R. & Kennard, O. (1982). Crystallographic evidence for the existence of C-H···O, C-H···N, and C-H···Cl hydrogen bonds. *J. Am. Chem. Soc.* **104**, 5063-5070.
13. Derewenda, Z. S., Lee, L. & Derewenda, U. (1995). The occurrence of C-H···O hydrogen bonds in proteins. *J. Mol. Biol.* **252**, 248-262.

14. Chothia, C. (1973). Conformation of twisted β-pleated sheets in proteins. *J. Mol. Biol.* **75**, 295-302.
15. Chou, K. C., Nemethy, G. & Scheraga, H. A. (1983). Role of interchain interactions in the stabilization of the right-handed twist of β-sheets. *J. Mol. Biol.* **168**, 389-407.
16. Yang, A. S. & Honig, B. (1995). Free energy determinants of secondary structure formation. II. Antiparallel β-sheets. *J. Mol. Biol.* **252**, 366-376.
17. MacCallum, P. H., Poet, R. & Milner-White, E. J. (1995). Coulombic attractions between partially charged main-chain atoms stabilise the right-handed twist found in most β-strands. *J. Mol. Biol.* **248**, 374-384.
18. Shamovsky, I. L., Ross, B. M. & Riopelle, R. J. (2000). Theoretical studies on the origin of β-sheet twisting. *J. Phys. Chem. sect. B,* **104**, 11296-11307.
19. Wang, L., O'Connell, T., Tropsha, A. & Hermans, J. (1996). Molecular simulations of β-sheet twisting. *J. Mol. Biol.* **262**, 283-293.
20. Raghavendra, K. & Sasisekharan, V. (1979). Conformational analysis of the right-hand twisted antiparallel β-structure. *Int. J. Pept. Protein Res.* **14**, 326-338.
21. Salemme, F. R. (1983). Structural properties of protein β-sheets. *Prog. Biophys. Mol. Biol.* **42**, 95-133.
22. Richardson, J. S. (1981). The anatomy and taxonomy of protein structures. *Advan. Protein Chem.* **34**, 167-339.
23. Fabiola, G. F., Krishnaswamy, S., Nagarajan, V. & Pattabhi, V. (1997). C-H···O hydrogen bonds in β-sheets. *Acta Crystallog. sect. D,* **53**, 316-320.
24. Desiraju, G. R. (1991). The C-H···O hydrogen bond in crystals: what is it? *Accts Chem. Res.* **24**, 290-296.
25. Vargas, R., Garza, J., Dixon, D. A. & Hay, B. P. (2000). How strong is the C^{α}-H···O═C hydrogen bond?. *J. Am. Chem. Soc.* **122**, 4750-4755.
26. Bernstein, F. C., Koetzle, T. F., Williams, G. J., Meyer, E. E., Brice, M. D., Rodgers, J. R. *et al*. (1977). The Protein Data Bank: a computer-based archival file for macromolecular structures. *J. Mol. Biol.* **112**, 535-542.
27. Hobohm, U., Scharf, M., Schneider, R. & Sander, C. (1992). Selection of representative protein datasets. *Protein Sci.* **1**, 409-417.
28. Engh, R. & Huber, R. (1991). Accurate bond and angle parameters for X-ray protein structure refinement. *Acta Crystallog. sect. A,* **47**, 392-400.
29. Press, W. H., Flannery, B. P., Teukolsky, S. A. & Vetterling, W. T. (1986). *Numerical Recipes*, Cambridge University Press, New York.
30. Brooks, B. R., Bruccoleri, R. E., Olafson, B. D., States, D. J., Swaminathan, S. & Karplus, M. (1983). CHARMM: a program for macromolecular energy minimisation and dynamics calculations. *J. Comput. Chem.* **4**, 187-217.
31. Word, M. J., Lovell, S. C., LaBean, T. H., Taylor, H. C., Zalis, M. E., Presley, B. K. *et al*. (1999). Visualizing and quantifying molecular goodness-of-fit: small-probe contact dots with explicit hydrogen atoms. *J. Mol. Biol.* **285**, 1711-1733.

Appendix

Analysis of Ramachandran plots

In antiparallel β-sheets, the Ramachandran plot of the non-H-bonded pair (see Figure 5(a) of the main text; slope −0.53; correlation coefficient −0.61) resembles the Ramachandran plot of the H-bonded pair (Figure 5(e) of the main text; slope −0.49; correlation coefficient −0.53). Both φ-ψ plots of the antiparallel β-sheets are weakly correlated with approximately the same slope, giving a consensus slope of −0.5 and a consensus φ-ψ range of ($-147^\circ < \phi < -110^\circ$; $119^\circ < \psi < 150^\circ$). The similarity between these two Ramachandran plots arises from the fact that we have taken the residues from the interior of the β-sheet. An interior β-sheet residue is simultaneously part of both an H-bonded and a non-H-bonded pair, and hence there is no physical difference between the two types of residues, even though the two distributions constitute two different sample sets.

In the antiparallel β-ribbon, the Ramachandran plot of the non-H-bonded pair (Figure 5(b) of the main text; slope −0.20; correlation coefficient 0.20) is different from the Ramachandran plot of the H-bonded pair (Figure 5(f) of the main text; slope −0.76; correlation coefficient −0.63). The φ-ψ angles of the H-bonded pair residues are correlated, whereas the φ-ψ angles of the non-H-bonded pair residues are not correlated. The two distributions are different, because H-bonded pair residues are physically distinct from non-H-bonded pair residues in the antiparallel β-ribbon.

If the main difference between antiparallel β-sheets and antiparallel β-ribbons is that β-sheet residues are shared between an H-bonded pair and a non-H-bonded pair, then we can interpret the consensus antiparallel β-sheet Ramachandran plot as the intersection of the H-bonded pair and non-H-bonded pair Ramachandran plots of the antiparallel β-ribbon. The intersection of the antiparallel β-ribbon H-bonded pair and non-H-bonded pair Ramachandran plot has a range in φ-ψ given by ($-142^\circ < \phi < -112^\circ$; $121^\circ < \psi < 149^\circ$). We calculate the slope of the intersection as the average of the slope of the H-bonded φ-ψ plot (−0.8) and of the non-H-bonded φ-ψ plot (−0.2), giving a slope of −0.5. This compares favourably with the consensus antiparallel β-sheet Ramachandran plot, which has a range in φ-ψ given by ($-147^\circ < \phi < -110^\circ$; $119^\circ < \psi < 150^\circ$) and a slope of −0.5. The idea that the conformation of antiparallel β-sheets is a subset of the conformation of antiparallel β-ribbons can be seen in that the significant correlations observed in the antiparallel β-ribbons (first column in Figures 4 and 8 of the main text) are observed also in the antiparallel β-sheet (third column in Figures 4 and 8 of the main text).

In parallel β-sheets, both the wide residue Ramachandran plot (Figure 5(i) of the main text; slope −0.22; correlation coefficient −0.27) and the narrow residue Ramachandran plot (Figure 5(m) of the main text; slope −0.18; correlation coefficient −0.20) are not correlated. However, the range of the distributions of the two Ramachandran plots are similar and the range of φ-ψ of the consensus Ramachandran plot is given by ($-135^\circ < \phi < -95^\circ$; $116^\circ < \psi < 142^\circ$). Unlike the antiparallel Ramachandran plots, the parallel β-sheet Ramachandran

plots are not correlated; therefore the consensus parallel Ramachandran plot is not correlated and only the range of the consensus parallel Ramachandran plot is a useful measure. The similarity between the two Ramachandran plots is due to the interior residues of the parallel β-sheet acting as both a narrow and wide residue in different inter-strand parallel pairs.

In the parallel β-ribbons, the Ramachandran plot of the wide residue (Figure 5(j) of the main text; slope −0.25; correlation coefficient −0.27) is different from the Ramachandran plot of the narrow residue (Figure 5(n) of the main text; slope −0.61; correlation coefficient −0.60). The ϕ-ψ angles of the narrow residue are weakly correlated, whereas the ϕ-ψ angles of the wide residue are not correlated. The intersection of ϕ-ψ plots of the narrow and wide residue has a range in ϕ-ψ of ($-138^\circ < \phi < -100^\circ$; $118^\circ < \psi < 156^\circ$), which compares well with the common parallel β-sheet ϕ-ψ range of ($-135^\circ < \phi < -95^\circ$; $116^\circ < \psi < 142^\circ$). The inter-strand parameters of the parallel pair in parallel β-sheets compare favourably with those of parallel β-ribbons (Table 1 of the main text). The conformation of the parallel β-sheet residues can be understood as the intersection of the conformations of the two residue types in the parallel β-ribbon.

Analysis of intra-strand interactions and ϕ-ψ

We have analysed the intra-strand distances that are parameterised by the ϕ-ψ dihedral angles of the backbone (Figure 2(b) of the main text), focusing specifically on the intra-strand $O\cdots H^\alpha$, $H\cdots H^\alpha$ and $O\cdots C^\beta$ distances. For these atom pairs, an observed close contact could be due to a van der Waals repulsion acting as a hard limit, to an inter-strand interaction, or to an intra-strand interaction. In a β-ribbon, a pair of intra-strand atoms can be located on the inner interface or an outer interface of the β-ribbon as indicated in Figure 1(d) and (e) of the main text. Inter-strand interactions will act only on the inner interface. For instance, the attraction of an O atom on the opposite strand forces the H and H^α atoms on the inner interface together into a steric contact (see below). However, there is no equivalent interaction that forces the H and H^α atoms together on the outer interface, resulting in a different distribution of the $d(H\cdots H^\alpha)$ distances on the outer interface compared to the distribution on the inner interface of the β-ribbon. If an inter-atomic contact is induced by an intra-strand interaction, then the same distribution of inter-atomic distances will be found on both the inner and outer interface of the β-ribbon.

Intra-strand $d(O\cdots H^\alpha)$ and ϕ

By fixing the covalent bond lengths and angles of the backbone (see Methods), the inter-atomic distance between O and H^α along the backbone is dependent on the ϕ angle (Figure 2(b) of the main text). This produces a curve of $d(O\cdots H^\alpha)$ *versus* ϕ, which has a minimum at $d(O\cdots H^\alpha) = 2.33$ Å and $\phi = 120^\circ$. The observed distributions of intra-strand $d(O\cdots H^\alpha)$ *versus* ϕ sit near the bottom of the curve in all β-ribbon residues (Figure 6 of the main text: (a) antiparallel non-H-bonded pair residue; (b) antiparallel H-bonded pair residue; (c) parallel wide residue; and (d) parallel narrow residues). As the distributions lie near the minimum, large variations in ϕ correspond to small deviations in $d(O\cdots H^\alpha)$.

The most striking property of the intra-strand $O\cdots H^\alpha$ distance is that $d(O\cdots H^\alpha) = 2.40(\pm 0.1)$ Å in all β-sheet residues (data not shown) and β-ribbon residues (Figure 6(a)-(d) of the main text). The fact that the same value of $d(O\cdots H^\alpha)$ is observed, both on the inside interface and the outside interface of the β-ribbons, suggests that this is an intra-strand effect. As $d(O\cdots H^\alpha)$ is correlated to ϕ, the restricted values of $d(O\cdots H^\alpha)$ could be constrained by any of the other intra-strand inter-atomic interactions that are parameterised by ϕ. However, of these intra-strand distances (Table 3 of the main text; where $d(O^{i-1}\cdots H^{\alpha,i})$ corresponds to the intra-strand $d(O\cdots H^\alpha)$ distance), only $d(O\cdots H^\alpha)$ is within range of a steric contact over the observed ϕ range of $-150^\circ < \phi < -90^\circ$, leaving $d(O\cdots H^\alpha)$ as the only plausible source of an intra-strand effect.

Given that O and H^α are polarised atoms (as indicated by the formation of the inter-strand $C^\alpha H^\alpha\cdots O$ hydrogen bond), there must be an intra-strand electrostatic interaction between the O and H^α, atoms. The question remains as to the strength of this interaction, which can be answered only by a detailed quantum mechanical calculation. However, two interesting measurements shed light on this question. First, the standard deviation of the $O\cdots H^\alpha$, distance is 0.1 Å in all cases. This standard deviation is comparable to that of H-bonded and covalent-bonded distances. Second, as $d(O\cdots H^\alpha) = 2.5$ Å of the inter-strand $C^\alpha H^\alpha\cdots O$ H-bond represents a significant interaction,[A1] the intra-strand values of $d(O\cdots H^\alpha) = 2.4$ Å suggests that the intra-strand $O\cdots H^\alpha$ interaction may be of comparable magnitude.

Fortunately, the conformation energy of β-strands using density functional theory bas been calculated by Shamovsky and co-workers.[A2] They found that ''$\cdots$ the rotational potential of ϕ in VIII [backbone with alanine sidechain] has a remarkably flat minimum between -90° and -150°.'' However, they did not give a physical mechanism for this minimum. As the range of $\phi(-150^\circ < \phi < -90^\circ)$ corresponds to $d(O\cdots H^\alpha) = 2.4(\pm 0.1)$ Å, we can re-interpret the results of the quantum mechanical calculation as a remarkably flat potential of the backbone for $d(O\cdots H^\alpha) = 2.4(\pm 0.1)$ Å. This supports the existence of an intra-strand $O\cdots H^\alpha$ non-bonded polar interaction.

Intra-strand $d(H\cdots H^{\alpha})$ and ψ

We also calculated the ideal curve of intra-strand $d(H\cdots H^{\alpha})$ as a function of ψ (Figure 2(b) of the main text), which has a minimum value of 2.22 Å at $\psi = 120^{\circ}$. The observed distributions of $d(H\cdots H^{\alpha})$ *versus* ψ also sit near the bottom of the curve in all β-ribbon residues (Figure 6 of the main text: (e) antiparallel non-H-bonded pair residue; (f) antiparallel H-bonded pair residue; (g) parallel wide residue; and (h) parallel narrow residues). However, the most striking feature is that in all cases, the distributions lie asymmetrically to the right of the minimum of the curve where the values of ψ are biased towards $\psi > 116^{\circ}$.

In the antiparallel β-ribbons, the distribution in $d(H\cdots H^{\alpha})$ *versus* ψ facing the inner interface (non-H-bonded pair; Figure 6(e) of the main text) is more constrained than the distribution facing the outer interface (H-bonded pair; Figure 6(f) of the main text). Similarly in parallel β-ribbons, the distribution of $d(H\cdots H^{\alpha})$ *versus* ψ facing the inner interface (wide residue; Figure 6(g) of the main text) is more constrained than the distribution facing the outer interface (narrow residue; Figure 6(h) of the main text). The values of inner $d(H\cdots H^{\alpha})$ in the parallel β-ribbons (2.29(±0.09) Å) and in the antiparallel β-ribbons (2.28(±0.07) Å) are both near the van der Waals[A3] contact distance of 2.17 Å, suggesting that the H and H^{α} atoms are in steric contact. As both H and H^{α} are positively charged atoms, another interaction must be forcing the two atoms together.

The formation of the bifurcated H-bond gives a plausible explanation for the $H\cdots H^{\alpha}$ steric contact observed on the inner interface of β-ribbons. The O atom in the bifurcated H-bond forms H-bonds with neighbouring H and H^{α}, atoms where the resultant electrostatic attraction of the O atom to the H and H^{α} atoms forces the two H-atoms together (Figure 2(c) of the main text). If forcing the H and H^{α} atoms together is the only constraint on the ψ angles, then restricting $d(H\cdots H^{\alpha})$ to 2.29(±0.09) Å would result in the restricted values of $90^{\circ} < \psi < 150^{\circ}$. However, observed ψ angles are always biased to the right-half of this region ($\psi > 116^{\circ}$). Another mechanism is required to account for this bias.

Intra-strand $d(O\cdots C^{\beta})$ and ψ

The asymmetry of the ψ angles with respect to the $d(H\cdots H^{\alpha})$ *versus* ψ curve is found for all residues in β-ribbons (Figure 6(i)-(l) of the main text) and β-sheets (data not shown), suggesting that this is an intra-strand effect. The intra-strand $O\cdots C^{\beta}$ distance is parameterised by the ψ dihedral angle (Figure 2(b) of the main text). By comparing the ideal curve of $d(O\cdots C^{\beta})$ *versus* ψ to the observed distributions, it can be seen that the values of $\psi > 116^{\circ}$ correlate to $d(O\cdots C^{\beta}) > 2.9$ Å in all β-ribbon residues (Figure 6 of the main text: (i) antiparallel non-H-bonded pair residue; (j) antiparallel H-bonded pair residue; (k) parallel wide residue; and (l) parallel narrow residues). Since the $O\cdots C^{\beta}$ van der Waals[A3] radius is 3.15 Å, the observed limit of $d(O\cdots C^{\beta}) = 2.9$ Å is consistent with the lower limit of a steric contact, suggesting that the bias of $\psi > 116^{\circ}$ is due to an intra-strand $O\cdots C^{\beta}$ steric clash destabilising residues with values of ψ in the region $<116^{\circ}$.

References

A1. Taylor, R. & Kennard, O. (1982). Crystallographic evidence for the existence of C-H···O, C-H···N, and C-H···Cl hydrogen bonds. *J. Am. Chem. Soc.* **104**, 5063-5070.

A2. Shamovsky, I. L., Ross, B. M. & Riopelle, R. J. (2000). Theoretical studies on the origin of β-sheet twisting. *J. Phys. Chem. sect. B*, **104**, 11296-11307.

A3. Word, M. J., Lovell, S. C., LaBean, T. H., Taylor, H. C., Zalis, M. E., Presley, B. K. *et al*. (1999). Visualizing and quantifying molecular goodness-of-fit: small-probe contact dots with explicit hydrogen atoms. *J. Mol. Biol*. **285**, 1711-1733.

Edited by J. Thornton

(Received 29 August 2001; received in revised form 17 December 2001; accepted 18 December 2001)